HAL open science

Abiotic degradation of highly branched isoprenoid alkenes and other lipids in the water column off East Antarctica

Jean-Francois Rontani, Lukas Smik, Simon Belt, Frederic Vaultier, Linda Armbrecht, Amy Leventer, Leanne Armand

To cite this version:

Jean-Francois Rontani, Lukas Smik, Simon Belt, Frederic Vaultier, Linda Armbrecht, et al.. Abiotic degradation of highly branched isoprenoid alkenes and other lipids in the water column off East Antarctica. Marine Chemistry, 2019, 210, pp.34-47. 10.1016/j.marchem.2019.02.004 . hal-02325661

HAL Id: hal-02325661

https://hal.science/hal-02325661

Submitted on 22 Oct 2021

HAL is a multi-disciplinary open access archive for the deposit and dissemination of scientific research documents, whether they are published or not. The documents may come from teaching and research institutions in France or abroad, or from public or private research centers.

L'archive ouverte pluridisciplinaire **HAL**, est destinée au dépôt et à la diffusion de documents scientifiques de niveau recherche, publiés ou non, émanant des établissements d'enseignement et de recherche français ou étrangers, des laboratoires publics ou privés.

Distributed under a Creative Commons Attribution - NonCommercial 4.0 International License

Version of Record: https://www.sciencedirect.com/science/article/pii/S0304420318302834
Manuscript_9a1394fb92059b8f013cb8b32cbfb201

Abiotic degradation of highly branched isoprenoid alkenes and other lipids in the water column off East Antarctica

Jean-François Rontani[a,*], Lukas Smik[b], Simon T. Belt[b], Frédéric Vaultier[a], Linda Armbrecht[c], Amy Leventer[d], Leanne K. Armand[e]

[a] *Aix Marseille Université, Université de Toulon, CNRS/INSU/IRD, Mediterranean Institute of Oceanography (MIO), UM 110, 13288 Marseille, France*

[b] *Biogeochemistry Research Centre, School of Geography, Earth and Environmental Sciences, University of Plymouth, Drake Circus, Plymouth, Devon PL4 8AA, UK*

[c] *Australian Centre for Ancient DNA, School of Biological Sciences, Faculty of Sciences, The University of Adelaide, Adelaide, South Australia, 5005, Australia*

[d] *Department of Geology, Colgate University, Hamilton, NY 13346, USA*

[e] *Research School of Earth Sciences, The Australian National University, Acton, Australian Capital Territory, 2601, Australia.*

* Corresponding author. Tel.: +33-4-86-09-06-02; fax: +33-4-91-82-96-41. *E-mail address*: jean-francois.rontani@mio.osupytheas.fr (J.-F. Rontani)

© 2019 published by Elsevier. This manuscript is made available under the CC BY NC user license
https://creativecommons.org/licenses/by-nc/4.0/

Abstract. In some previous studies, the ratio between a di-unsaturated highly branched isoprenoid (HBI) lipid termed $IPSO_{25}$ and a structurally related tri-unsaturated counterpart (HBI III) (viz. $IPSO_{25}$/HBI III) has been used as a proxy measure of variable sea ice cover in the Antarctic owing to their production by certain sea ice algae and open water diatoms, respectively. To investigate this further, we quantified selected lipids and their photo- and autoxidation products in samples of suspended particulate matter (SPM) collected at different water depths in the polynya region west of the Dalton Iceberg Tongue (East Antarctica). The results obtained confirm the high efficiency of photo- and autoxidation processes in diatoms from the region. The systematic increase of the ratio $IPSO_{25}$/HBI III with water depth in the current samples appeared to be dependent on the sampling site and was due to both (i) a relatively higher contribution of ice algae to the deeper samples resulting from their increased aggregation and therefore higher sinking rate, or (ii) a stronger abiotic degradation of HBI III during settling through the water column. Analyses of samples taken from the water-sediment interface and some underlying near-surface sediments revealed a further increase of the ratio $IPSO_{25}$/HBI III, indicative of further differential oxidation of the more unsaturated HBI. Unfortunately, specific oxidation products of HBI III could not be detected in the strongly oxidized SPM and sediment samples, likely due to their lability towards further oxidation. In contrast, oxidation products of HBI III were detected in weakly oxidized samples of phytoplanktonic cells collected from Commonwealth Bay (also East Antarctica), thus providing more direct evidence for the involvement of photo- and/or autoxidation of HBI III in the region. This oxidative alteration of the ratio $IPSO_{25}$/HBI III between their source and sedimentary environments might need to be considered more carefully when using this parameter for palaeo sea ice reconstruction purposes in the Antarctic.

Key words: East Antarctica; Suspended particulate matter; Near-surface sediments; Lipids; Photo- and autoxidation; Alteration of $IPSO_{25}$/HBI III ratio; Paleoceanographic implications.

1. Introduction

Sea ice plays a central role in the overall climate structure of the Polar Regions (Thomas, 2017). Amongst its various well known attributes, its high albedo (reflectivity) means that sea ice serves as an efficient regulator of incoming solar radiation to the surface oceans. Further, the physical structure of sea ice provides a physical barrier to the exchange of gas, heat and moisture between the polar oceans and the atmosphere. It is also an important contributor to near-surface stratification, bottom-water formation and ventilation, in particular (e.g. Dickson et al., 2007 and references therein). From a biogeochemical perspective, nutrient release during ice melt in spring, coupled with surface layer stratification and increasing light and temperature, often leads to intense open water phytoplankton production, especially along the retreating ice edge or the so-called marginal ice zone (MIZ) (Smith and Nelson 1986; Smith, 1987; Sakshaug et al., 2009; Perette et al., 2011).

Understanding the well documented abrupt changes in sea ice in the polar regions (Stroeve et al., 2012; Fetterer et al., 2016, Serreze et al., 2016; Walsh et al., 2017) requires more detailed knowledge of how it has changed in the past in response to other climatic drivers. A common approach to achieve this is through the analysis of so-called sea ice proxies present in marine sediment archives. The majority of these proxies possess some kind of biological origin, although there are others (e.g. de Vernal et al., 2013 and references therein). In the Antarctic, the identification of certain ice-associated diatoms in polar marine sediments has a long history of use for palaeo sea ice determinations (Armand et al., 2017). However, the growth habitat of the target species are normally more closely associated with the open waters of the MIZ rather than that of sea ice itself (Leventer, 1998; Leventer et al., 2008). On the other hand, those diatoms that bloom within the sea ice

host (i.e. the strictly sympagic community), are often under-represented in sedimentary records (Leventer, 2013).

Over the last decade or so, a number of diatom-derived lipid biomarkers have emerged as useful complementary sea ice proxies to the more traditional micropaleontological-based approaches. Thus a mono-unsaturated highly branched isoprenoid (HBI) termed IP_{25} (Ice Proxy with 25 carbon atoms; Belt et al., 2007) has emerged as a useful proxy for seasonal Arctic sea ice (for reviews, see Belt and Muller, 2013; Belt, 2018), while a di-unsaturated structural homolog of IP_{25} – sometimes referred to as HBI II (**1**; see appendix) – appears to be a suitable counterpart for the Antarctic. A recent source identification and the near ubiquity of the diene **1** in near-coastal sediments from around the Antarctic continent has led to its recent designation as $IPSO_{25}$ (Ice Proxy for the Southern Ocean with 25 carbon atoms; Belt et al., 2016) by analogy with IP_{25}. A further, tri-unsaturated HBI, often termed HBI III (**2**), is also showing potentially as a biomarker proxy indicator of the MIZ in both Polar Regions. Thus, enhanced concentrations of HBI III (**2**) have been observed in surface sediments from the MIZ of the Barents Sea in the Arctic (Belt et al., 2015) and in surface waters of the MIZ in East Antarctica (Smik et al., 2016) and the Scotia Sea (Schmidt et al., 2018) shortly following sea ice melt. As a result, some palaeo sea ice records based on HBI II (hereafter referred to as $IPSO_{25}$) (**1**) and HBI III (**2**) for the Antarctic have appeared in recent years (Barbara et al., 2010,2013,2016; Denis et al., 2010; Collins et al., 2013; Etourneau et al., 2013; Campagne et al., 2015,2016). A general interpretation of greater sea ice extent for relatively high $IPSO_{25}$ (**1**) compared to HBI III (**2**), and more open water conditions for increased HBI III (**2**) concentrations has been applied. In some of these studies, variability in the ratio **1/2** has been used as a qualitative measure of changes to sea ice cover; however, this assumption has, as yet, not been validated through comparison of surface

sediment biomarker data with known overlying sea ice conditions in the same way as for IP_{25} (and HBI III (**2**) in some cases) in the Arctic (see Belt, 2018 for a recent review). Nonetheless, such interpretations are consistent with the data reported by Smik et al. (2016) following analysis of $IPSO_{25}$ (**1**) and HBI III (**2**) in surface waters from regions of variable sea ice cover from East Antarctica, with highest concentrations found in the summer sea ice zone and MIZ, respectively. Similar findings have also been reported for surface water samples from the Scotia Sea (Schmidt et al., 2018). However, the extent to which the surface water distributions of $IPSO_{25}$ (**1**) and HBI III (**2**) are replicated in the underlying sediments for palaeo sea ice reconstruction purposes was not investigated in the initial study by Smik et al. (2016).

To provide further insight to this, here we carried out analysis of further water samples from the polynya region proximal to the Dalton Ice Tongue in East Antarctica with the primary aim of determining any variability of the ratio **1/2** with water depth, and to reconcile outcomes through the identification of pathway-specific oxidation products of common phytoplankton lipids as indicators of well-known degradation processes (i.e. bacterial degradation, photooxidation and autoxidation). Further evidence for the oxidation of such lipids was obtained through the analysis of near-surface sediment material collected from the main study region and from filtered phytoplankton samples collected from Commonwealth Bay (also East Antarctica).

2. Materials and methods

2.1. Sampling

Water samples were obtained as part of the NBP1402 cruise aboard the RVIB *Nathaniel B Palmer* in February–March 2014 as described previously (Smik et al., 2016;

see also NBP1402 Scientific Cruise Report, 2014, Sabrina Coast: Marine record of cryosphere–ocean dynamics (467 pages) for further details) (http://www.marinegeo.org/tools/search/data/field/NBPalmer/NBP1402/docs/NBP1402CruiseReport_Final.pdf). For the current study, we focused on those locations that had experienced seasonal sea ice cover within the polynya region west of the Dalton Iceberg Tongue (East Antarctica). At each of the 12 sampling sites (Fig. 1), surface (0–10 m), sub-surface (chlorophyll *a* maximum; ca. 25–60 m) and deep (ca. 500–1100 m) water samples were obtained from CTD rosettes. At the five stations where we carried out lipid degradation studies, the surface CTD samples had already been used for native lipid analyses so we used water obtained from the ship's intake line (ca. <10 m); near-surface and deep water samples were obtained from the CTD rosettes as per the other stations. In each case, 1.5–3.0 l of sampled water was filtered onto 25 mm Whatman GF/F filters (as supplied), wrapped in aluminium foil and stored frozen (-80°C). Sample data are detailed in Supplementary Table 1. Megacoring was conducted using a Bowers and Connelly MegaCorer, with 12 10-cm diameter core tubes, for sampling an undisturbed sediment water interface. Surface water above the core tops and a layer of diatomaceous 'fluff' were pipetted off the top of the core tubes and stored frozen (-80°C). Sediment material from the cores was extruded at 0.5 to 2 cm intervals, depending on the core depth.

Three samples of phytoplankton cells (CB, AS607 and AS608) were collected in Commonwealth Bay (East Antarctica, 66°56S; 142°27E) during the IPEV-COCA2012 cruise in January 2012. Surface waters were sampled using a 25-µm ring net deployed from the R/V Astrolabe. Concentrated phytoplankton cell suspensions (ranging from 2.6 to 1.1 mg d.w. ml^{-1}) were stored frozen (-20 °C) prior to freeze drying and analysis.

2.2. Sample treatment

152 Lipids from all of the CTD samples, the waters above the sediment cores and the
153 diatomaceous 'fluff' were extracted and analyzed as described previously by Smik et al.
154 (2016). This treatment involved addition of internal standards (9-octyl-8-heptadecene for
155 HBI quantification, 5α-androstan-3β-ol for Δ^5-sterol quantification and nonadecanoic acid
156 for fatty acid quantification), saponification (5% KOH (9:1 v/v MeOH/H_2O); 70 °C; 60
157 min) and separation of non-saponifiable (hexane 3x2 ml) and saponifiable fractions (+1 ml
158 HCl; hexane (3x2 ml)). For sediments, ca. 1 g of freeze-dried material was extracted by
159 sonication (dichloromethane/methanol; 2:1 v/v, 3x2 ml) to obtain a total organic extract
160 (TOE). Subsequent purification of the unsaponifiable fraction/TOE by open column
161 chromatography (SiO_2) afforded HBIs (elution with hexane; 5 column volumes) and
162 sterols (elution with hexane-methyl acetate (4:1, v/v; 5 column volumes). In addition,
163 saturated non-polar components of TOEs were removed using silver-ion chromatography
164 (Belt et al., 2015).
165 Treatment of the filtered water samples from the five stations selected for lipid
166 oxidation product analyses and phytoplankton material collected from Commonwealth Bay
167 involved a different treatment. Following addition of MeOH (25 ml) and reduction with
168 excess $NaBH_4$ (70 mg, 30 min) of labile hydroperoxides to alcohols, which are more
169 amenable to analysis using gas chromatography–mass spectrometry (GC-MS), water (25
170 ml) and KOH (2.8 g) were added and the resulting mixture saponified by refluxing (2 h).
171 After cooling, the mixture was acidified (HCl, 2 N) to pH 1 and extracted with
172 dichloromethane (DCM; 3 x 20 ml). The combined DCM extracts were dried over
173 anhydrous sodium sulfate, filtered and concentrated via rotary evaporation at 40°C to give
174 total lipid extracts (TLEs).
175 A different treatment (Rontani et al., 2018) was employed to estimate the relative
176 proportions of hydroperoxides and their ketonic and alcoholic degradation products in

177 phytoplankton samples from Commonwealth Bay. This involved ultrasonic extraction of
178 lipids with chloroform-MeOH-water (1:2:0.8, v/v/v), separation of the supernatant by
179 centrifugation at 3500G, evaporation to dryness, and division of the residue into two equal
180 parts. The first sub-sample was acetylated in acetic anhydride-pyridine (1:2, v/v) overnight,
181 which converted hydroperoxides to the corresponding ketones (Mihara and Tateba, 1986),
182 and then saponified. The second sub-sample was reduced with $NaBD_4$ and saponified.
183 Comparison of the amounts of alcohols present after acetylation and $NaBD_4$ reduction
184 made it possible to estimate the amount of hydroperoxides and alcohols present in the
185 samples, while deuterium labeling (via $NaBD_4$ reduction) allowed us to estimate the
186 proportion of ketones in the samples.
187
188 *2.3. Derivatization*
189 For all samples containing hydroxylic components, an aliquot was dissolved in 300
190 µl pyridine/bis(trimethylsilyl)trifluoroacetamide (BSTFA, Supelco; 2:1, v:v) and silylated
191 (1 h) at 50 °C. After evaporation to dryness under a stream of N_2, the derivatized residue
192 was dissolved in a mixture of ethyl acetate and BSTFA (to avoid desilylation) and
193 analyzed by GC–MS, GC-QTOF or GC–MS/MS.
194
195 *2.4. Assignment and quantification of lipids*
196 Native lipids were identified and quantified using GC–MS in total ion current (TIC)
197 or selected ion monitoring (SIM) mode using a Hewlett-Packard 5890 Series II gas
198 chromatograph, fitted with a 30 m fused silica HP_{5ms} column (0.25 mm i.d., 0.25 µm film)
199 coupled to a 5970 Series Mass Selective Detector (MSD) (Belt et al., 2012). Individual
200 lipids (and their derivatised products) were identified on the basis of their characteristic
201 GC retention indices (e.g. RI_{HP5ms} 2082 and 2044 for $IPSO_{25}$ and HBI III, respectively) and

202 mass spectra (Belt, 2018), together with comparison of both parameters with those
203 obtained from purified standards (Smik et al., 2016). Quantification of individual lipids
204 was achieved first by manual integration of GC–MS peak areas, division of these by those
205 of the respective internal standards, and normalization of the resulting ratios using
206 instrumental response factors obtained for each lipid (Belt et al., 2014; Smik et al., 2016).
207 These normalised ratios were then multiplied by the mass of the internal standard and
208 finally converted to their corresponding seawater concentrations using the volume of water
209 filtered or mass of sediment extracted. All analytical data can be found in Supplementary
210 Table 1.
211
212 *2.5. Assignment and quantification of lipid oxidation products*
213 Lipid oxidation products were identified by comparison of retention times, accurate
214 masses and mass spectra with those of standards and quantified (calibration with external
215 standards) using gas chromatography–electron ionization quadrupole time of flight mass
216 spectrometry (GC-QTOF). GC-QTOF analyses were carried out with an Agilent
217 7890B/7200A GC-QTOF System (Agilent Technologies, Parc Technopolis - ZA
218 Courtaboeuf, Les Ulis, France). A cross-linked 5% phenyl-methylpolysiloxane (Macherey
219 Nagel; Optima 5-MS Accent) column (30 m × 0.25 mm, 0.25 μm film thickness) was
220 employed. Analyses were performed with an injector operating in pulsed splitless mode at
221 280 °C and the oven temperature programmed from 70 °C to 130 °C at 20 °C min^{-1}, then to
222 250 °C at 5 °C min^{-1}, and then to 300 °C at 3 °C min^{-1}. The carrier gas (He) was
223 maintained at 0.69×10^5 Pa until the end of the temperature program. Instrument
224 temperatures were 300 °C for the transfer line and 230 °C for the ion source. Accurate
225 mass spectra were obtained across the range *m/z* 50-700 at 4 GHz. The QTOF-MS

226 instrument provided a typical resolution ranging from 8009 to 12252 from *m/z* 68.9955 to
227 501.9706. Perfluorotributylamine (PFTBA) was utilized for daily MS calibration.
228
229 *2.6. Assignment and quantification of HBI oxidation products*
230 Quantification of HBI oxidation products was carried out using an Agilent 7850-A
231 gas chromatograph connected to an Agilent 7010-QQQ mass spectrometer working in
232 multiple reaction monitoring (MRM) mode. The following conditions were employed: 30
233 m x 0.25 mm (i.d.) fused silica column coated with HP-5MS (Agilent; film thickness: 0.25
234 µm); oven programmed from 70 to 130 °C at 20 °C min^{-1}, then to 250 °C at 5 °C min^{-1} and
235 then to 300 °C at 3 °C min^{-1}; carrier gas (He), 1.0 bar; injector (splitless), 250 °C; electron
236 energy, 70 eV; source temperature, 230 °C; quadrupole temperature, 150 °C; scan range
237 m/z 40-700; collision energy, ranging from 5 to 15 eV; collision flow, 1.5 ml min^{-1} (N_2);
238 quench flow, 2.25 ml min^{-1} (He); cycle time, 0.2 s. Oxidation products were assigned by
239 comparison of retention times and mass spectra with those of standards. Due to the
240 presence of two highly photo-reactive tri-substituted double bonds (C-7/20 and C-9/10) in
241 HBI III (**2**), it was not possible to quantify its primary oxidation products directly using
242 standards, since they are not accumulated due to rapid further oxidation (Rontani et al.,
243 2014a). We therefore quantified photoproducts of a related HBI triene (**3**) (possessing only
244 one reactive tri-substituted double bond (C-9/10); see appendix) as an external standard
245 and estimated the quantities of oxidation products from HBI III (**2**) by applying a
246 correction factor (Rontani et al., 2014b).
247
248 *2.7. Standard compounds*
249 The synthesis of 3-methylidene-7,11,15-trimethylhexadecan-1,2-diol (phytyldiol) (**7**)
250 was described previously by Rontani and Aubert (2005). (8-11)-Hydroperoxyhexadec-(8-

251 10)-enoic acids (*Z* and *E*) (**36**-**41**) and (8-11)-Hydroperoxyoctadec-(8-10)-enoic (*Z* and *E*)
252 (**30**-**35**) acids were produced by Fe^{2+}/ascorbate-induced autoxidation (Loidl-Stahlhofen and
253 Spiteller, 1994) of palmitoleic and oleic acids, respectively. Subsequent reduction of these
254 different hydroperoxides in methanol with excess $NaBH_4$ afforded the corresponding
255 hydroxyacids. 3,6-Dihydroxy-cholest-4-ene (**18**) (employed for sterol photooxidation
256 estimates) was obtained from Maybridge Ltd. Treatment of sitosterol (**42**) with meta-
257 chloroperoxy-benzoic acid in dry DCM yielded a mixture of 5α,6α-and 5β,6β-epoxides.
258 Heating of these epoxides in the presence of water afforded the corresponding 24-
259 ethylcholesta-3β,5α,6β-triol (**43**) (Holland and Diakow, 1979). $IPSO_{25}$ (**1**) and HBI triene
260 **3** were purified from cultures of *Haslea ostrearia* (Belt et al., 1996; Johns et al., 1999),
261 while HBI III (**2**) was obtained from a culture of *Pleurosigma intermedium* (Belt et al.,
262 2000). Photosensitized oxidation products (hydroperoxides) of these HBI alkenes were
263 produced in pyridine in the presence of haematoporphyrin as photosensitizer and then
264 reduced with $NaBH_4$ to the corresponding alcohols (Rontani et al., 2014a).
265
266 *2.8 Diatom taxonomy*
267 Diatom identification and enumeration were carried out for selected water and
268 sediment samples. Specifically, three water samples of 200 ml each were collected at
269 CTD015 (5, 40, 563 m). Overlying bottom water (100 µl), diatomaceous fluff (50 µl) and
270 sediment samples were collected from MC061. Sediment was also collected from MC045.
271 The water samples were immediately fixed with Lugol's solution (~0.5 ml). Back at the
272 laboratory, the preserved water samples were concentrated (CTD015) or diluted (MC061)
273 into Utermöhl chambers to a final volume of 3 ml. After sedimentation of 48 h, a minimum
274 total of 400 cells (including microphyto- and microzooplankton live at the time of
275 preservation), were identified and counted following the Utermöhl method (Utermöhl,

276 1958) at a magnification of 400x under an inverted microscope (Olympus IMT-2, Japan).
277 Microplankton were identified to species level where possible using appropriate taxonomic
278 literature (Hasle, 1965; Tomas, 1997; Scott and Marchant, 2005, Kim et al. 2013). Final
279 counts were converted to cells l^{-1}. Sediment samples were dried at 50 °C. Quantitative
280 slides were made using a settling method (Scherer, 1994). Approximately 5 ml of water
281 and hydrogen peroxide was added to several mg of each sample, and the samples were
282 placed on a warming tray at 50 °C for 2–3 days. After complete reaction and removal of
283 organic material, the samples were poured into water-filled 1 l beakers and allowed to
284 settle onto coverslips. The coverslips were mounted on glass slides using Norland Optical
285 Adhesive #61 cured under UV light. These quantitative slides were used for assessment of
286 the diatom assemblage, by identification and counting of a minimum of 400 diatom valves
287 along cross-slide transects, at a magnification of 1000x. Counting followed the method
288 described by Schrader and Gersonde (1978) and Crosta and Koc (2007). Diatom
289 concentration (diatom valves per gram) and relative abundance (percentage) of diatom
290 species were calculated.

291 For the purposes of the current investigation, we determined the distribution of three
292 common *Fragilariopsis* spp. to provide a semi-quantitative assessment of the relative
293 contribution from sea ice-associated (*F. curta* and *F. cylindrus*) and open water (*F.*
294 *kerguelensis*) diatoms. (Armand et al., 2005; Crosta et al., 2005; Crosta et al., 2008). Thus,
295 the ratio (*F. curta* + *F. cylindrus*)/*F. kerguelensis* was determined (Table 2).

296

297 **3. Results and discussion**

298 The identification and quantification of the various lipids and their degradation
299 products are described here according to the individual lipid classes at each sampling
300 location. The sequence of presentation is arranged so as to first provide sufficient evidence

for the oxidation state of the lipids, in order that the variability in the ratio of $IPSO_{25}$ (**1**)/HBI III (**2**) can then be put into context.

3.1. Lipids and their degradation products in water samples from west of the Dalton Iceberg Tongue

3.1.1. Chlorophyll phytyl side-chain

In addition to phytol (**4**), which mainly arises from the hydrolysis of the chlorophyll phytyl side-chain during alkaline hydrolysis, significant amounts of 3,7,11,15-tetramethylhexadecanoic acid (phytanic acid) (**5**), 3,7,11,15-tetramethylhexadec-1-en-ol-3 (isophytol) (**6**) and 3-methylidene-7,11,15-trimethylhexadecan-1,2-diol (phytyldiol) (**7**) could also be detected in the different samples. However, phytanic acid (**5**) was not quantified in the present work due to its lack of specificity. Indeed, this isoprenoid acid is also formed during the aerobic and anaerobic bacterial degradation of phytol (Rontani and Volkman, 2003) and the grazing of phytoplankton (Prahl et al., 1984).

In contrast, there have been very few reports of the presence of isophytol (**6**) in the marine environment (Fang et al., 2006), so its relatively high proportion compared to phytol (**1**) in some samples (Table 1) is potentially surprising. Isophytol (**6**) may be formed in sediments either by enzyme-catalyzed allylic rearrangement during bacterial degradation of phytol under denitrifying conditions (Rontani et al., 1999), or by clay-catalyzed dehydration of phytol (de Leeuw et al., 1974). It is interesting to note that relatively high proportions of isophytol were also recently observed after $NaBH_4$-reduction and alkaline hydrolysis of phytoplanktonic cells collected from Commonwealth Bay, Antarctica (Rontani and Galeron, 2016). In order to explain this observation, it was proposed that

325 allylation (Berkessel, 2009) of the chlorophyll phytyl side-chain by peroxyl radicals could
326 result in the formation of the precursor 3-peroxy-3,7,11,15-tetramethylhexadec-1-ene (**8**),
327 with subsequent reduction to isophytol (**6**) (Fig. 2) (Rontani and Galeron, 2016). The
328 absence of the initial reduction step employed here (i.e. using $NaBH_4$) during conventional
329 treatment of environmental samples is likely at the origin of the very few reports of
330 isophytol (**6**) in previous studies. In any case, the high values of the ratio isophytol/phytol
331 observed at station 25, and to a lesser extent at station 28B (Table 1), attest to the presence
332 of high concentrations of peroxides, and thus of a strong photo- or autoxidation state of
333 POM.

334 The formation of phytyldiol (**7**) results from initial Type II photosensitized oxidation
335 (i.e. involving singlet oxygen ($^1O_2$)) of the chlorophyll phytyl side-chain and subsequent
336 hydrolysis of the photoproducts thus formed (Rontani et al., 1994). On the basis of its high
337 specificity and widespread occurrence in the environment (Cuny and Rontani, 1999), this
338 diol can be used as a specific tracer of chlorophyll photodegradation. Further, Cuny et al.
339 (2002) proposed that the amount of chlorophyll photodegradation in the marine
340 environment could be estimated from the so-called Chlorophyll Phytyl side-chain
341 Photodegradation Index (CPPI) derived from the molar ratio phytyldiol/phytol. Using this
342 approach, the highest photooxidation state of POM was confirmed as being at station 25
343 and the lowest at station 32 (<1%, not included in the figure) (Fig. 3).
344

345 3.1.2. Sterols

346 The major sterols in the filtered water sample were 24-norcholest-5,22*E*-dien-3β-ol
347 (22-dehydrocholesterol) (**10**), cholest-5-en-3β-ol (cholesterol) (**11**), 24-methylcholesta-
348 5,22*E*-dien-3β-ol (*epi*-brassicasterol) (**12**), 24-methylcholesta-5,24(28)-dien-3β-ol (24-
349 methylenecholesterol) (**13**) and 24-ethylcholest-7-en-3β-ol (22-dihydrocondrillasterol) (**14**)

350 (Supplementary Table 1). 22-Dehydrocholesterol (**10**) has been found in diatoms and
351 notably in *Thalassiosira aff. antarctica* (Rampen et al., 2007). Although cholesterol (**11**)
352 may be derived from diatoms or Prymnesiophycean algae (Volkman, 1986), its dominance
353 generally suggests an important contribution of zooplanktonic faecal material to the
354 samples. Indeed, it is well known that zooplankton convert much of the sterols produced
355 by algae into cholesterol (**11**) (Volkman et al., 1980; Prahl et al., 1984). *Epi*-brassicasterol
356 (**12**) and 24-methylenecholesterol (**13**) are major constituents of several diatom species
357 (Lee et al., 1980) including sea ice diatoms (Belt et al., 2018). However, it may be noted
358 that *epi*-brassicasterol (**12**) is also present in some dinoflagellates and in many haptophytes
359 (Volkman, 1986, 2003). The unusual sterol 22-dihydrochondrillasterol (**14**) was detected
360 previously in some Chlorophyceae (Martin-Creuzburg et al., 2011; Martin-Creuzburg and
361 Merkel, 2016). The sterol profiles observed in these samples (Supplementary Table 1) are
362 thus typical of mixed assemblages of diatoms, Prymnesiophytes and Chlorophytes.
363 Type II photosensitized oxidation of Δ^5-sterols produces mainly unstable Δ^6-5α-
364 hydroperoxides with low amounts of Δ^4-6α/β-hydroperoxides (Smith, 1981). Here, we
365 selected Δ^4-6α/β-hydroperoxides as tracers of photooxidation of Δ^5-sterols due to their
366 high specificity and relative stability (Rontani et al., 2009; Christodoulou et al., 2009).
367 These compounds were quantified after $NaBH_4$ reduction to the corresponding diols and
368 photooxidation percentage was obtained from the equation: photooxidation % = (Δ^4-stera-
369 6α/β-diols % × (1+0.3)/0.3) (Christodoulou et al., 2009). The values obtained for *epi*-
370 brassicasterol (**12**) and 24-methylenecholesterol (**13**) (the two main algal sterols present in
371 the samples analyzed) are shown in Fig. 3. Photooxidation of these two sterols exhibits the
372 same general trend as that seen for chlorophyll, with the highest photooxidation state
373 observed at station 25 (Fig. 3). Interestingly, as observed previously in the Arctic (Rontani
374 et al., 2012; 2014a), photodegradation processes appeared to have acted more intensively

375 on 24-methylenecholesterol (**13**) (mainly arising from diatoms) than on *epi*-brassicasterol
376 (**12**) (arising from diatoms and/or Prymnesiophytes). These differences confirm the higher
377 efficiency of Type II photosensitized oxidation processes in diatoms compared to
378 Prymnesiophytes.

379 Stanols constitute useful indicators of bacterial degradation of Δ^5-sterols (Gagosian
380 et al., 1982; de Leeuw and Baas, 1986; Wakeham, 1989). We thus quantified the ratio 24-
381 methyl-5α-cholest-22*E*-en-3β-ol (*epi*-brassicastanol) (**15**)/*epi*-brassicasterol (**12**) to
382 indicate the extent of bacterial degradation of algal material. (Note: the ratio 24-methyl-
383 5α-cholest-24(28)-en-3β-ol (**16**)/24-methylenecholesterol (**13**) could not be quantified due
384 to co-elution of the stanol **16** with the isobaric campesterol (**17**)). The values of the ratio
385 *epi*-brassicastanol (**15**)/*epi*-brassicasterol (**12**) (Table 1) show only a weak increase with
386 depth suggesting that bacterial degradation processes acted only weakly on algal material.
387

388 3.1.3. Fatty acids

389 The fatty acid content of the SPM samples is characterized by a very low content of
390 polyunsaturated fatty acids (PUFAs) and notably of $C_{18:4}$ (**19**), $C_{20:5}$ (**20**) and $C_{22:6}$ (**21**)
391 acids, which are typical for marine plankton (Kattner et al., 1983). Instead, the dominant
392 fatty acids are the saturated and monounsaturated fatty acids (MUFAs) (i.e. $C_{14:0}$ (**22**),
393 $C_{16:1\omega7}$ (palmitoleic acid) (**23**), $C_{16:0}$ (palmitic acid) (**24**), $C_{18:1\omega9}$ (oleic acid) (**25**), $C_{18:1\omega7}$
394 (vaccenic acid) (**26**) and $C_{18:0}$ (**27**)) (Supplementary Table 1). The reactivity of unsaturated
395 fatty acids with respect to auto- and photooxidative processes increases, logically, with the
396 number of double bonds (Frankel, 1998; Rontani et al., 1998). The very low amounts of
397 PUFAs is therefore suggestive of intense photo- or autoxidation of the samples. In order to
398 confirm this, the oxidation products of MUFAs (oleic and palmitoleic acids) (**25** and **23**)
399 were quantified since they are sufficiently stable in the marine environment to act as

markers of these abiotic degradative processes (Marchand and Rontani, 2001, 2003). Photo- and autoxidation of monounsaturated fatty acids affords mixtures of isomeric allylic hydroperoxyacids (Frankel, 1998). Based on the specific formation of *cis* isomers by autoxidation (Porter et al., 1995), the relative importance of photooxidation and autoxidation can easily be distinguished by quantifying the respective hydroxyacids that result from $NaBH_4$-reduction of these compounds (Marchand and Rontani, 2001). The results obtained (Fig. 4) show a clear difference in reactivity between palmitoleic (**23**) and oleic (**25**) acids. Indeed, photo- and autoxidation states appeared to be considerably higher in the case of palmitoleic acid (**23**) (the main MUFA of diatoms, Fahl and Kattner, 1993; Leu et al., 2010) compared to oleic acid (**25**) (dominant in Prymnesiophytes, Rossi et al., 2006). These outcomes are consistent with previous observations of more efficient photo- and autoxidation processes in diatoms than in Prymnesiophytes (Rontani et al., 2012; 2014b). Such differences in reactivity were attributed previously to the involvement of intra-cellular compartmentalization effects, which may significantly modify the reactivity of lipids towards autoxidative and photooxidative processes according to their location in phytoplanktonic cells (Rontani, 2012).

The palmitoleic (**23**)/palmitic acid (**24**) ratio is often employed to follow diatom blooms (Pedersen et al., 1999; Reuss and Poulsen, 2002). Due to the strong oxidation of palmitoleic acid (**23**) observed in some of our samples (Fig. 4), we employed the ratio (Σ palmitoleic acid (**23**) and its oxidation products)/palmitic acid (**24**) to estimate the relative proportion of diatom in the mixed phytoplankton assemblages. Using this approach, we observed a relatively high proportion of (strongly oxidized) diatoms in the surface water sample of station 25 and an increase in their proportion with water depth at station 28B (Table 1).

3.1.4. Cutin components

Relatively high amounts of 9,16-dihydroxyhexadecanoic (**29**) and 10,16-dihydroxyhexadecanoic (**28**) acids were observed in some samples (Table 1). These compounds are well-known depolymerisation products of cutins (insoluble polyester polymers) present in the outer layer of the epidermal cells of primary plant tissues, such as leaves) (Deas and Holloway, 1977; Kolattukudy, 1977, 1980). The presence of such compounds is very surprising since the Antarctic biome is an unfavorable environment for higher plant growth. Only two native phanerogams, *Deschampsia antarctica* Desv. and *Colobanthus quitensis* (Kunth) Bartl., occur in Antarctica to almost 69°S (Smith 1994). The high concentrations of dihydroxyacids **28** and **29** detected in some sub-surface water samples (Table 1) is therefore attributed to the accumulation of low density debris of such plants, probably resulting from inflow of near-surface water masses carrying terrestrial material. In contrast, the occurrence of these compounds due to sediment resuspension seems unlikely due to their absence in the deeper water column samples.

3.1.5. HBI alkenes

The two HBI lipids, $IPSO_{25}$ (**1**) and HBI III (**2**), reported previously by Smik et al. (2016) in the surface water samples described here, were also present in each of the sub-surface and deep water samples investigated for the first time within the current study. Although there was some variability in the absolute and relative concentrations of these HBIs between the surface and sub-surface samples, The $IPSO_{25}$ (**1**)/HBI III (**2**) ratio was mainly slightly higher in the majority of the sub-surface samples compared to the surface water counterparts, with CTD-004 and -014 the only exceptions. More striking changes to this ratio were observed with the corresponding deep water samples, however, with mean

449 (i.e. across all samples) relative enhancements in $IPSO_{25}$ (**1**)/HBI III (**2**) of ca. 8 and 6
450 when compared with the surface and sub-surface samples, respectively (Table 1).

451 The systematic increase of the ratio **1/2** with depth (Table 1) may potentially be
452 attributed to: (i) a relatively higher contribution of ice algae (and thus $IPSO_{25}$ (**1**)) to the
453 deeper samples resulting from their stronger aggregation and therefore higher sinking rate,
454 or (ii) a stronger abiotic degradation of HBI III (**2**) during settling through the water
455 column. One characteristic of sea ice algae is their ability to produce high amounts of
456 extracellular polymeric substances (EPS); the production of which facilitates the
457 attachment of algae to their substrate (sea ice) but also allows the formation of aggregates
458 of algal cells (Riebesell, 1991; Alldredge et al., 1993; Passow, 2002), thus shortening their
459 residence time within the euphotic zone. In the case of station 28B, the simultaneous
460 increase of the ratios **1/2** and (Σ palmitoleic acid (**23**) and its oxidation products)/palmitic
461 acid (**24**) with depth (Table 1) suggests a dominance of aggregated ice diatom material in
462 the deepest SPM sample.

463 Photo- and autoxidation of $IPSO_{25}$ (**1**) were previously studied in vitro (Rontani et
464 al., 2011; 2014a). Based on its very low degradation rates (resulting from the poor
465 reactivity of its two terminal double bonds (i.e. at C6-17 and C23-24) towards $^1O_2$ and free
466 radicals), it is feasible that this diene (**1**) could be largely unaffected by abiotic oxidation
467 within the water column of the oceans, at least in comparison with some more unsaturated
468 lipids, or those containing more reactive double bonds. Indeed, HBI III (**2**) possesses two
469 tri-substituted double bonds (i.e. at C7–20 and C9–10), both of which are more reactive
470 towards $^1O_2$ (Frimer, 1983) than the two double bonds in $IPSO_{25}$. In addition, the relative
471 positions of these two double bonds in HBI III (**2**) creates a bis-allylic methylene group (at
472 C-8) that can lose a hydrogen atom even more readily (Yin et al., 2011). HBI III (**2**) is thus
473 very sensitive towards photo- and autoxidation processes and exhibits degradation rates

close to those of PUFAs (Rontani et al., 2014a). On the basis of the very intense abiotic alteration of these fatty acids in the samples investigated here (see section 3.1.3), a similar oxidation of HBI III (**2**) was thus expected. However, we were not able to detect the previously identified primary oxidation products of HBI III (**2**) (Rontani et al., 2014a), probably due to their further oxidation to polar and oligomeric compounds, which are not generally detectable using the GC–MS methods employed here. This conclusion is consistent with the strong photo- and autoxidation states of palmitoleic acid (**23**) observed in these samples (Fig. 4) and the differences of reactivity observed previously between HBI III (**2**) and this acid in diatom cells ($k_{photo\ HBI\ III}/k_{photo\ palmitoleic\ acid} \approx 4$ and $k_{auto\ HBI\ III}/k_{auto\ palmitoleic\ acid} > 10$) (Rontani et al., 2011; 2014a).

In order to provide further evidence for the influence of autoxidative processes upon the ratio **1/2**, we measured it, together with the autoxidation state of sitosterol (**42**) (estimated on the basis of 3β,5α,6β-trihydroxysitosterol (**43**) as previously proposed by Christodoulou et al. (2009)) and palmitoleic acid (**23**) in the water column samples from station 32 (T32/CTD015) and in two near-surface sediment samples from nearby locations (MC45 and MC61; Fig. 1), with one of these (MC61) located directly at the station where the CTD015 samples were taken. The ratio **1/2** was also measured in the surface waters recovered from the top of the MC61 sediment core and in the suspension of diatomaceous 'fluff' taken at the water-sediment interface, thereby providing a near-continuous depth sequence from surface waters to underlying sediments. Although sitosterol (**42**) is commonly associated with higher plants ((Lütjohann, 2004), it is also present in phytoplankton, and notably in diatoms (Volkman, 1986; 2003). Due to the absence of lipid signatures of terrestrial material in the water samples collected at station 32 and in the sediments from nearby locations, the presence of sitosterol (**42**) in these samples was thus attributed to an algal origin. The results obtained (Table 2) show a clear increase in both

the ratio **1/2** and the autoxidation state of algal material with water depth and then into the surface sediments (Table 2). The failure to detect oxidation products of sitosterol in the water column samples is attributed to the relatively poor chromatographic properties of the only partially silylated (at positions 3 and 6) triol **43**, which hinders its detection at low concentrations.

Although we do not currently have detailed taxonomic data from all sampling stations/types, we do have data from the station for which we have lipid profiles from both the water column and underlying Megacore (viz. CTD015 & MC61). The most striking feature is the consistent decrease in the ratio (*F. curta* + *F. cylindrus*)/*F. kerguelensis* through the water column, the water-sediment interface and then into the sub-surface sediment (Table 2), suggesting a progressive decrease in the relative contribution of sea ice-associated and open-water diatoms. However, this conclusion is contrary to what might be inferred from the (increasing) $IPSO_{25}$ (**1**) /HBI III (**2**) ratio, suggesting that changes in the latter, at some locations, are determined more by the enhanced degradation of HBI III (**2**)(relative to $IPSO_{25}$) as shown from the lipid data described above; the caveat being that the aforementioned *Fragilariopsis* spp. are not known HBI-producers. We also assume that the water column data derived from samples taken in a single sampling season are also representative of multi-annual accumulation that the sediment samples likely reflect. Unfortunately, the known sources of $IPSO_{25}$ and HBI III (**2**) were of too low abundance for more direct comparisons between lipid and taxonomic distributions to be made for these samples. Interestingly, a positive relationship between $IPSO_{25}$ (**1**)/HBI III (**2**) and the ratio *F. curta*/*F. kerguelensis* (i.e., a slight modification to our diatom ratio) was reported in a previous downcore sediment study from the region (Massé et al., 2011), suggesting that the modifications to the former described herein for the water column and water-sediment interface may not necessarily have an adverse impact on its use as a proxy measure of sea

ice change in palaeo records, especially for qualitative purposes. Further studies comparing these two approaches will, however, be required, before the generality of this observation can be confirmed, and the most reliable use of $IPSO_{25}$/HBI III as a proxy measure of sea ice change can be deciphered.

3.2. Phytoplanktonic material from Commonwealth Bay (East Antarctica)

To demonstrate the efficiency of photo- and autoxidation processes on HBI III (**2**) in this region, more generally, we also analysed phytoplanktonic cells collected from surface waters of Commonwealth Bay (also East Antarctica; see Fig. 1). In this weakly oxidized material (oxidation percentage of palmitoleic acid (**23**) < 5%), MRM analyses allowed us to detect the HBI alcohols **44–48** (Figs. 5B and 6B, Table 3). The assignment of these compounds was confirmed by comparison with the MRM chromatograms of standards obtained by photo- and autoxidation of HBI III (**2**) (Figs. 5A and 6A) (Rontani et al., 2014b). Alcohol **48** is produced specifically by photooxidation of HBI III (**2**), while alcohols **44–47** result from both its photo- and autoxidation (Rontani et al., 2014a). On the basis of the detection of these oxidation products in a weakly oxidized phytoplanktonic sample from Commonwealth Bay, the strong increase of the ratio $IPSO_{25}$ (**1**)/HBI III (**2**) observed in the deeper SPM samples from stations 25, 27, 32 and 34 and in near-surface sediments from the polynya region west of the Dalton Iceberg Tongue (Tables 1 and 2) may be thus attributed to an intense photo- and/or autoxidation of HBI III (**2**) within the water column, with further autoxidation of HBI III (**2**), relative to $IPSO_{25}$ (**1**), at the water-sediment interface and in the oxic layer of the underlying sediment.

During the $NaBH_4$-reduction step employed to avoid thermal degradation of hydroperoxides during the subsequent saponification reaction, the sum of hydroperoxides and their degradation products (alcohols and ketones) was obtained via quantification of

549 their respective alcohols. Two different treatments were employed (acetylation and
550 saponification *vs* $NaBD_4$-reduction and saponification) (see Section 2.2) in order to
551 specifically quantify hydroperoxides and their main degradation products (i.e. alcohols and
552 ketones). The results obtained (summarized in Table 4) show that a substantial proportion
553 (ca. 55–81%) of HBI III (**2**) oxidation products were still present as hydroperoxides.
554 Interestingly, the decrease in unlabeled phytol (**4**) concentration (5–20%) observed
555 when the treatment of phytoplanktonic cells involved acetylation and saponification
556 instead of $NaBD_4$-reduction and saponification, provides further evidence for the formation
557 pathway of isophytol (**6**) proposed previously (Rontani and Galeron, 2016) (Fig. 2).
558 Indeed, this decrease likely results from the presence of 1-peroxy-3,7,11,15-
559 tetramethylhexadec-3-ene (**9**), which is formed by allylic rearrangement of its isomer **8**
560 (Fig. 2).
561

562 ## 4. Conclusions

563 Selected lipids and their oxidation products were quantified in SPM samples
564 collected at different water depths in the polynya region west of the Dalton Iceberg Tongue
565 (East Antarctica). The sterol profiles were typical of mixed assemblages of diatoms,
566 prymnesiophytes and chlorophytes. Surprisingly, some samples contained
567 depolymerisation products of cutins, the presence of which was attributed to the
568 accumulation of low-density debris of the two phanerogams present in Antarctica.
569 We identified an intense photo- and autoxidation of unsaturated diatom components
570 (e.g. palmitoleic acid (**23**), 24-methylenecholesterol (**13**), chlorophyll phytyl side-chain
571 (**4**)), but not of HBI III (**2**)**,** despite its known reactivity towards such processes, likely due
572 to its susceptibility towards further oxidation. However, oxidation products of HBI III (**2**)

could be detected in weakly oxidized SPM samples collected from Commonwealth Bay (East Antarctica), clearly demonstrating the oxidation of this lipid in this region.

The systematic increase of the ratio $IPSO_{25}$ (**1**)/HBI III (**2**) observed with depth in the water column and in some underlying sediments thus appears to result, in part, from an intense and preferential abiotic degradation of the HBI III (**2**) due to a combination of photo- and autoxidation processes (Fig. 7). At one sampling site, the increase in the $IPSO_{25}$ (**1**)/HBI III (**2**) ratio with depth was opposite to that of the ratio of selected sea ice-associated versus open-water diatoms, suggesting that the differential biomarker degradation was a dominant factor. However, for another sampling site, the increase in the $IPSO_{25}$ (**1**)/HBI III (**2**) ratio appeared to be more influenced by the accumulation of ice algal material, although we do not yet have the complementary taxonomic data to confirm this.

Distinguishing between these two factors will require more detailed and combined lipid and taxonomic analysis in the future. In the meantime, it is evident from the results presented here, that the differential degradation of $IPSO_{25}$ (**1**) and HBI III (**2**) in the water column and in near-surface sediments (at least) can impact on the ratio between these two HBIs between their source and sedimentary environments. The latter should be taken into account when using this parameter for palaeo sea ice reconstruction purposes in the Antarctic. The extent to which the $IPSO_{25}$ (**1**)/HBI III (**2**) ratio reflects established proxy measures of past sea ice change (e.g., the ratio of certain *Fragilariopsis* spp. as described herein) will require more studies of both parameters in further downcore records from the Antarctic.

Acknowledgements

The FEDER OCEANOMED (N° 1166-39417) is acknowledged for the funding of the apparatus employed. Thanks are due to the scientific party and crew of cruise NBP1402; the project (P.I. A. Leventer) was funded by NSF ANT-1143836. We also thank G. Massé for the donation of the phytoplankton samples collected in the Commonwealth Bay during the IPEV-COCA2012 cruise funded by IPEV (1010-ICELIPIDS program) and ANR (CLIMICE program). We thank two anonymous referees for their useful and constructive comments.

References

Alldredge, A.L., Passow, U., Logan, B.E., 1993. The abundance and significance of a class of large, transparent organic particles in the ocean. Deep-Sea Research Part I-Oceanographic Research Papers 40, 1131-1140.

Armand, L., Crosta, X., Romero, O., Pichon, J.J., 2005. The biogeography of major diatom taxa in Southern Ocean sediments.1. Sea ice related species. Palaeogeography, Palaeoclimatology, Palaeoecology 223, 93–126.

Armand, L.K., Ferry, A., Leventer, A., 2017. Advances in palaeo sea ice estimation. In: Thomas, D.N. (Ed.), Sea Ice. John Wiley & Sons Ltd, Chichester, pp. 600–629.

Barbara, L., Crosta, X., Massé, G., Ther, O., 2010. Deglacial environments in eastern Prydz Bay, East Antarctica. Quaternary Science Reviews 29, 2731–2740.

Barbara, L., Crosta, X., Schmidt, S., Massé, G., 2013. Diatoms and biomarkers evidence for major changes in sea ice conditions prior the instrumental period in Antarctic Peninsula. Quaternary Science Reviews 79, 99–110.

Barbara, L., Crosta, X., Leventer, A., Schmidt, S., Etourneau, J., Domack, E., Massé, G., 2016. Environmental responses of the Northeast Antarctic Peninsula to the Holocene climate variability, Paleoceanography, 31, 131–147.

Belt, S.T., Cooke, D.A., Robert, J.-M., Rowland, S.J., 1996. Structural characterisation of widespread polyunsaturated isoprenoid biomarkers: A C_{25} triene, tetraene and pentaene from the diatom *Haslea ostrearia* Simonsen. Tetrahedron Letters 37, 4755–4758.

Belt, S.T., Allard, W.G., Massé, G., Robert, J.-M., Rowland, S.J., 2000. Highly branched isoprenoids (HBIs): identification of the most common and abundant sedimentary isomers. Geochimica et Cosmochimica Acta 64, 3839–3851.

Belt, S.T., Massé, G., Rowland, S.J., Poulin, M., Michel, C., LeBlanc, B., 2007. A novel chemical fossil of palaeo sea ice: IP_{25}. Organic Geochemistry 38, 16–27.

Belt, S.T., Müller, J., 2013. The Arctic sea ice biomarker IP_{25}: a review of current understanding, recommendations for future research and applications in palaeo sea ice reconstructions. Quaternary Science Reviews 79, 9–25.

Belt, S.T., Brown, T.A., Ampel, L., Cabedo-Sanz, P., Fahl, K., Kocis, J.J., Masse, G., Navarro-Rodriguez, A., Ruan, J., Xu, Y., 2014. An inter-laboratory investigation of the Arctic sea ice biomarker proxy IP_{25} in marine sediments: key outcomes and recommendations. Climate of the Past 10, 155–166.

Belt, S.T., Cabedo-Sanz, P., Smik, L., Navarro-Rodriguez, A., Berben, S.M.P., Knies, J., Husum, K., 2015. Identification of paleo Arctic winter sea ice limits and the marginal ice zone: Optimised biomarker-based reconstructions of late Quaternary Arctic sea ice. Earth and Planetary Science Letters 431, 127–139.

Belt, S.T., Smik, L., Brown, T.A., Kim, J.H., Rowland, S.J., Allen, C.S., Gal, J.K., Shin, K.H., Lee, J.I., Taylor, K.W.R., 2016. Source identification and distribution reveals

the potential of the geochemical Antarctic sea ice proxy $IPSO_{25}$. Nature Communications 7, 12655.

Belt, S.T., Brown, T.A., Smik, L., Assmy, P., Mundy, C.J., 2018. Sterol identification in floating Arctic sea ice algal aggregates and the Antarctic sea ice diatom *Berkeleya adeliensis*. Organic Geochemistry 118, 1–3.

Belt, S.T., 2018. Source-specific biomarkers as proxies for Arctic and Antarctic sea ice. Organic Geochemistry 125, 273-295.

Berkessel, A., 2014. Science of Synthesis: Houben-Weyl Methods of Molecular Transformations, Vol. 38: Peroxides, Georg Thieme Verlag, p. 75.

Brown, T.A., Belt, S.T., Tatarek, A., Mundy, C.J., 2014c. Source identification of the Arctic sea ice proxy IP_{25}. Nature Communications 5, 4197.

Campagne, P., Costa, X., Houssais, M.N., Swingedouw, D., Schmidt, S., Martin, A., Devred, E., Capo, S., Marieu, V., Closset, I., Massé, G., 2015 Glacial ice and atmospheric forcing on the Mertz Glacier Polynya over the past 250 years. Nature Communications 6, 6642.

Campagne, P., Crosta, X., Schmidt, S., Houssais, M.N., Ther, O., Massé, G., 2016. Sedimentary response to sea ice and atmospheric variability over the instrumental period off Adélie Land, East Antarctica. Biogeosciences 13, 4205–4218.

Christodoulou S., Marty J.-C., Miquel J.-C., Volkman J.K., Rontani J.-F., 2009. Use of lipids and their degradation products as biomarkers for carbon cycling in the northwestern Mediterranean Sea. Marine Chemistry 113, 25-40.

Collins, L.G., Allen, C.S., Pike, J., Hodgson, D.A., Weckström, K., Massé, G., 2013. Evaluating highly branched isoprenoid (HBI) biomarkers as a novel Antarctic sea-ice proxy in deep ocean glacial age sediments. Quaternary Science Reviews 79, 87–98.

Crosta, X., Koc, N., 2007. Diatoms: From micropaleontology to isotope geochemistry, in: Methods in Late Cenozoic Paleoceanography, Hilaire-Marcel, C. and de Vernal, A. (Eds.), Elsevier, Amsterdam, the Netherlands, pp. 327–369.

Crosta, X., Romero, O., Armand, L., Pichon, J.J., 2005. The biogeography of major diatom taxa in Southern Ocean sediments. 2. Open Ocean related species. Palaeogeography, Palaeoclimatology, Palaeoecology 223, 66–92.

Crosta, X., Denis, D., Ther, O., 2008. Sea ice seasonality during the Holocene, Adelie Land, East Antarctica. Marine Micropaleontology 66, 222–232.

Cuny, P., Rontani, J.-F., 1999. On the widespread occurrence of 3-methylidene-7,11,15-trimethylhexadecan-1,2-diol in the marine environment: a specific isoprenoid marker of chlorophyll photodegradation. Marine Chemistry 65, 155-165.

Cuny, P., Marty, J.-C., Chiaverini, J., Vescovali, I., Raphel, D., Rontani, J.-F., 2002. One-year seasonal survey of the chlorophyll photodegradation process in the Northwestern Mediterranean Sea. Deep-Sea Research II 49, 1987-2005.

Deas, A.H.B., Holloway, P.J., 1977. The intermolecular structure of some plant cutins. In: Tevini, M., Lichtenthaler, H. (Eds.), Lipids and Lipid Polymers in Higher Plants. Springer, Berlin, pp. 293-299.

Denis, D., Crosta, X., Barbara, L., Massé, G., Renssen, H., Ther, O., Giraudeau, J., 2010. Sea ice and wind variability during the Holocene in East Antarctica: insight on middle-high latitude coupling. Quaternary Science Reviews 29, 3709–3719.

de Leeuw, J.W., Correia, V.A., Schenck, P.A., 1974. On the decomposition of phytol under simulated geological conditions and in the top-layer of natural sediments. In: Tissot, B., Bienner, F. (Eds.), Advances in Organic Geochemistry 1973. Editions Technip, Paris, pp. 993–1004.

de Leeuw, J.W., Baas, M., 1986. Early-stage diagenesis of steroids. In: Johns, R.B. (Ed.), Biological Markers in the Sedimentary Record. Elsevier, Amsterdam, pp. 101-123.

de Vernal, A., Gersonde, R., Goosse, H., Seidenkrantz, M.-S., Wolff, E.W., 2013. Sea ice in the paleoclimate system: the challenge of reconstructing sea ice from proxies – an introduction. Quaternary Science Reviews 79, 1–8.

Dickson, R., Rudels, B., Dye, S., Karcher, M., Meincke, J., Yashayaev, I., 2007. Current estimates of freshwater flux through Arctic and subarctic seas. Progress in Oceanography 73, 210–230.

Etourneau, J., Collins, L.G., Willmott, V., Kim, J.H., Barbara, L., Leventer, A., Schouten, S., Sinninghe Damsté, J.S., Bianchini, A., Klein, V., Crosta, X., Massé, G., 2013. Holocene climate variations in the western Antarctic Peninsula: evidence for sea ice extent predominantly controlled by changes in insolation and ENSO variability. Climate of the Past 9, 1431–1446.

Fahl, K., Kattner, G., 1993. Lipid content and fatty acid composition of algal communities in sea-ice and water from Weddell Sea (Antarctica). Polar Biology 13, 405-409.

Fang, J., Chan, O., Joeckel, R.M., Huang, Y., Wang, Y., Bazylinski, D.A., Moorman, T.B., Ang Clement, B.J., 2006. Biomarker analysis of microbial diversity in sediments of a saline groundwater seep of Salt Basin, Nebraska. Organic Geochemistry 37, 912-931.

Fetterer F., Knowles K., Meier W.N., Savoie M., 2016. Sea Ice Index. ver.2 NSIDC: National Snow and Ice Data Center. Boulder, Colorado (https://doi.org/10.7265/N5736NV7) [Digital Media, updated daily].

IPCC, 2013: Summary for Policymakers. In: Climate Change 2013: The Physical Science Basis. Contribution of Working Group I to the Fifth Assessment Report of the Intergovernmental Panel on Climate Change [Stocker, T.F., D. Qin, G.-K. Plattner, M.

Tignor, S.K. Allen, J. Boschung, A. Nauels, Y. Xia, V. Bex and P.M. Midgley (eds.)]. Cambridge University Press, Cambridge, United Kingdom and New York, NY, USA.

Frankel, E.N., 1998. Lipid Oxidation. The Oily Press, Dundee.

Frimer, A.A., 1979. The reaction of singlet oxygen with olefins: the question of mechanism. Chemical Review 79, 359-387.

Gagosian, R.B., Smith, S.O., Nigrelli, G.E., 1982. Vertical transport of steroid alcohols and ketones measured in a sediment trap experiment in the equatorial Atlantic Ocean. Geochimica et Cosmochimica Acta 46, 1163-1172.

Hasle, G.R., 1965. *Nitzschia* and *Fragilariopsis* species studied in the light and electron microscopes III. The genus *Fragilariopsis.* Skr. Norske Vidensk-Akad. I. Mat.-Nat. Kl. Ny Serie 21, 1–49.

Holland, H.L., Diakow, P.R.P., 1979. Microbial hydroxylation of steroids. 5. Metabolism of androst-5-en-3,17-dione and related compounds by *Rhizopus arrhizus* ATCC 11145. Canadian Journal of Chemistry 57, 436-440.

Johns, L., Wraige, E.J., Belt, S.T., Lewis, C.A., Massé, G., Robert, J.M., Rowland, S.J., 1999. Identification of a C_{25} highly branched isoprenoid (HBI) diene in Antarctic sediments, Antarctic sea-ice diatoms and cultured diatoms. Organic Geochemistry 30, 1471–1475.

Kattner, G., Cercken, G., Eberlein, K., 1983. Development of lipid during a spring bloom in the northern North Sea. I. Particulate fatty aclds. Marine Chemistry 14, 149-162.

Kim, S.Y., Choi, J.K., Dolan, J.R., Shin, H.C., Lee, S., Yang, E.J., 2013. Morphological and ribosomal DNA-based characterization of six Antarctic ciliate morphospecies from the Amundsen Sea with phylogenetic analyses. Journal of Eukaryotic Microbiology 60, 497-513.

Kolattukudy, P.E., 1977. Lipid polymers and associated phenols, their chemistry, biosynthesis, and role in pathogenesis, Recent Advances in Phytochemistry 77, 185-246.

Kolattukudy, P.E., 1980. Cutin, suberin and waxes. In: Stumpf, P.K., Conn, E.E. (Eds.), The Biochemistry of Plants, vol. 4. Academic Press, Davis, pp. 571–645.

Lee, C., Gagosian, R.B., Farrington, J.W., 1980. Geochemistry of sterols in sediments from Black Sea and the southwest African shelf and slope, Organic Geochemistry 2, 103-113.

Leventer, A., 2013. The fate of Antarctic "sea ice diatoms" and their use as paleoenvironmental indicators. In: Lizotte, M.P., Arrigo, K.R. (Eds.), Antarctic Sea Ice: Biological processes, Interactions and Variability. American Geophysical Union, pp. 121–137.

Leventer, A., Armand, L., Harwood, D.M., Jordan, R., Ligowski, R., 2008. New approaches and progress in the use of polar marine diatoms in reconstructing sea ice distribution. Papers in the Earth and Atmospheric Sciences. Paper 287.

Leventer, A., 1998. The fate of sea ice diatoms and their use as paleoenvironmental indicators. In: Lizotte, M.P. and Arrigo, K.R. (Eds.), Antarctic Sea Ice: Biological Processes, AGU Research Series 73, Washington, D.C., pp. 121–137.

Leu, E., Wiktor, J., Soreide, J.E., Berge, J., Falk-Petersen, S., 2010. Increased irradiance reduces food quality of sea ice algae. Marine Ecology Progress Series 411, 49-60.

Loidl-Stahlhofen, A., Spiteller, G., 1994. α–Hydroxyaldehydes, products of lipid peroxidation. Biochimica et Biophysica Acta 1211, 156-160.

Lütjohann, D., 2004. Sterol autoxidation: from phytosterols to oxyphytosterols. British Journal of Nutrition 91, 3-4.

765 Marchand, D., Rontani, J.-F., 2001. Characterisation of photooxidation and autoxidation
766 products of phytoplanktonic monounsaturated fatty acids in marine particulate matter
767 and recent sediments. Organic Geochemistry 32, 287-304.
768 Marchand, D., Rontani, J.-F., 2003. Visible light-induced oxidation of lipid components of
769 purple sulfur bacteria: a significant process in microbial mats. Organic Geochemistry
770 34, 61-79.
771 Martin-Creuzburg, D., Beck, B., Freese, H.M., 2011. Food quality of heterotrophic bacteria
772 for *Daphnia magna*: evidence for a limitation by sterols. FEMS Microbiology 76,
773 592-601.
774 Martin-Creuzburg, D., Merkel, P., 2016. Sterols of freshwater microalgae: potential
775 implications for zooplankton nutrition. Journal of Plankton Research 38, 865-877.
776 Mihara, S., Tateba, H., 1986. Photosensitized oxygenation reactions of phytol and its
777 derivatives. The Journal of Organic Chemistry 51, 1142-1144.
778 Passow, U., 2002. Transparent exopolymer particles (TEP) in aquatic environments.
779 Progress in Oceanography 55, 287-333.
780 Pedersen, L., Jensen, H.M., Burmeister, A.D., Hansen, B.W., 1999. The significance of
781 food web structure for the condition and tracer lipid content of juvenile snail fish
782 (Pisces: Liparis spp.) along 65–728N off West Greenland. Journal of Plankton
783 Research 21, 1593-1611.
784 Perette, M., Yool, A, Quartly, G.D., Popova, E.E., 2011. Near-ubiquity of ice-edge blooms in
785 the Arctic. Biogeosciences 8, 515–524.
786 Porter, N.A., Caldwell, S.E., Mills, K.A., 1995. Mechanisms of free radical oxidation of
787 unsaturated lipids. Lipids 30, 277-290.

Prahl, F.G., Eglinton, G., Corner, E.D.S., O'Hara, S.C.M., Forsberg, T.E.V., 1984. Changes in plant lipids during passage through the gut of *Calanus*. Journal of the Marine Biological Association of the United Kkingdom 64, 317-334.

Reuss, N., Poulsen, L.K., 2002. Evaluation of fatty acids as biomarkers for a natural plankton community. A field study of a spring bloom and a post-bloom period off West Greenland. Marine Biology 141, 423-434.

Riebesell U., Schloss I., Smetacek V., 1991. Aggregation of algae released from melting sea ice-implications for seeding and sedimentation. Polar Biology 11,239-248.

Rampen, S.W., Abbas, B.A., Schouten, S., Sinninghe Damsté, J.S., 2010. A comprehensive study of sterols in marine diatoms (Bacillariophyta): implications for their use as tracers for diatom productivity. Limnology and Oceanography 55, 91–105.

Rontani, J.-F., Grossi, V., Faure, F., Aubert, C., 1994. ''Bound'' 3-methylidene-7,11,15-trimethylhexadecan-1,2-diol: a new isoprenoid marker for the photodegradation of chlorophyll-a in seawater. Organic Geochemistry 21, 135-142.

Rontani, J.-F., Cuny, P., Grossi, V., 1998. Identification of a pool of lipid photoproducts in senescent phytoplanktonic cells. Organic Geochemistry 29, 1215-1225.

Rontani, J.-F., Bonin, P., Volkman, J.K., 1999. Biodegradation of free phytol by bacterial communities isolated from marine sediments under aerobic and denitrifying conditions. Applied and Environmental Microbiology 65, 5484–5492.

Rontani, J.-F., Volkman, J.K., 2003. Phytol degradation products as biogeochemical tracers in aquatic environments. Organic Geochemistry 34, 1-35.

Rontani, J.-F., Aubert, C., 2005. Characterization of isomeric allylic diols resulting from chlorophyll phytyl side chain photo- and autoxidation by electron ionization gas chromatography/mass spectrometry. Rapid Communications in Mass Spectrometry 19, 637-646.

Rontani, J.-F., Zabeti, N., Wakeham, S.G., 2009. The fate of marine lipids: Biotic vs. abiotic degradation of particulate sterols and alkenones in the Northwestern Mediterranean Sea. Marine Chemistry 113, 9-18.

Rontani, J.-F., Belt, S.T., Vaultier, F., Brown, T.A., 2011. Visible light-induced photo-oxidation of highly branched isoprenoid (HBI) alkenes: a significant dependence on the number and nature of the double bonds. Organic Geochemistry 42, 812-822.

Rontani, J.-F., 2012. Photo- and free radical-mediated oxidation of lipid components during the senescence of phototrophic organisms. In: T. Nagata Ed., Senescence. Intech, Rijeka, pp. 3-31.

Rontani, J.-F., Charriere, B., Forest, A., Heussner, S., Vaultier, F., Petit, M., Delsaut, N., Fortier, L., Sempéré, R., 2012. Intense photooxidative degradation of planktonic and bacterial lipids in sinking particles collected with sediment traps across the Canadian Beaufort Shelf (Arctic Ocean). Biogeosciences 9, 4787-4802.

Rontani, J.-F., Charrière, B., Sempéré, R., Doxaran, D., Vaultier, F., Vonk, J.E., Volkman, J.K., 2014a. Degradation of sterols and terrigenous organic matter in waters of the Mackenzie Shelf, Canadian Arctic. Organic Geochemistry 75, 61-73.

Rontani, J.-F., Belt, S., Vaultier, F., Brown, T., Massé, G., 2014b. Autoxidative and photooxidative reactivity of highly branched isoprenoid (HBI) alkenes. Lipids, 49(5), 481-494.

Rontani, J.-F., Galeron, M.-A., 2016. Autoxidation of chlorophyll phytyl side-chain in senescent phototrophic organisms: a potential source of isophytol in the environment. Organic Geochemistry 97, 37-40.

Rontani, J.-F., Amiraux, R., Lalande, C., Babin, M., Kim, H.-R., Belt, S.T., 2018. Use of palmitoleic acid and its oxidation products for monitoring the degradation of ice algae in Arctic waters and bottom sediments. Organic Geochemistry 124, 88-102.

Rossi, S., Sabates, A., Latasa, M., reyes, E., 2006. Lipid biomarkers and trophic linkages between phytoplankton, zooplankton and anchovy (*Engraulis encrasicolus*) larvae in the NW Mediterranean. Journal of Plankton Research 28, 551-562.

Sakshaug, E., Johnsen, G., Kristiansen, S., von Quillfeldt, C., Rey, F., Slagstad, D., Thingstad, F., 2009. Phytoplankton and primary production. In: Sakshaug, E., Johnsen, G., Kovacs, K. (Eds), Ecosystem Barents Sea. Tapir Academic Press, Trondheim, pp.167–208.

Scherer, R.P., 1994. A new method for the determination of absolute abundance of diatoms and other silt-sized sedimentary particles. Journal of Paleolimnology 12 (1), 171–178.

Schmidt, K., Brown, T.A., Belt, S.T., Ireland, L.C., Taylor, K.W.R., Thorpe, S.E., Ward, P., Atkinson, A., 2018. Do pelagic grazers benefit from sea ice? Insights from the Antarctic sea ice proxy $IPSO_{25}$. Biogeosciences 15, 1987– 2006.

Schrader, H.J., Gersonde, R., 1978. Diatoms and silicoflagellates. In: Zachariasse, A. (Ed.), Micropaleontological Counting Methods and Techniques - An Exercise on Eight Meters Section of the Lower Pliocene of Capo Rossello, Sicily. Utrecht Micropaleontology Bulletin, 17, pp. 129–176.

Scott, F., Marchant, H.J., 2005. Antarctic Marine Protists 1st ed. F. Scott and H. J. Marchant, eds., Canberra, Hobart: Australian Biological Resources Study and Australian Antarctic Division.

Serreze, M.C., Stroeve, J., Barrett, A.P., Boisvert, L.N., 2016. Summer atmospheric circulation anomalies over the Arctic Ocean and their influence on September sea ice extent. A cautionary tale. Journal of Geophysical Research: Atmospheres 121, 11463–11485.

Smik, L., Belt, S.T., Lieser, J.L., Armand, L.K., Leventer, A., 2016. Distributions of highly branched isoprenoid alkenes and other algal lipids in surface waters from East

Antarctica: Further insights for biomarker-based paleo sea-ice reconstruction. Organic Geochemistry 95, 71–80.

Smith, L.L., 1981. The autoxidation of cholesterol. Plenum Press, New York, pp. 119-132.

Smith, R.I.L., 1994. Vascular plants as bioindicators of regional warming in Antarctica. Oecologia 99, 322-328.

Smith, W.O., 1987. Phytoplankton dynamics in marginal ice zones. Oceanography and Marine Biology 25, 11–38.

Smith, W.O., Jr., Nelson, D.M., 1986. The importance of ice-edge blooms in the Southern Ocean. Biosciences 36, 251–257.

Stroeve, J.C., Serreze, M.C., Holland, M.M., Kay, J.E., Malanik, J., Barrett, A.P., 2012. The Arctic's rapidly shrinking sea ice cover: a research synthesis. Climate Change 110, 1005–1027.

Thomas, D.N., 2017. Sea ice 3rd ed. Wiley-Blackwell: pp 664.

Tomas, C.R., 1997. Identifying marine phytoplankton, San Diego: Academic Press.

Utermöhl, H., 1958. Zur Vervollkommnung der quantitativen Phytoplankton-Methodik. Internationale Vereinigung für theoretische und angewandte Limnologie: Mitteilungen 9, 1–38.

Volkman, J.K., Corner, E.D.S., Eglinton, G., 1980. Transformations of biolipids in the marine food web and in underlying bottom sediments, Colloque International du Centre National de la Recherche Scientifique 293, 185-197.

Volkman, J.K., 1986. A review of sterol markers for marine and terrigenous organic matter. Organic Geochemistry 9, 83-99.

Volkman, J.K., 2003. Sterols in microorganisms. Applied Microbiology and Biotechnology 60, 495-506.

887 Walsh, J.E., Fetterer, F., Scott Stewart, J., Chapman, W.L., 2017. A database for depicting
888 Arctic sea ice variations back to 1850. Geographical Review 107, 89–107.
889 Wakeham, S.G., 1989. Reduction of stenols to stanols in particulate matter at oxic-anoxic
890 boundaries in seawater. Nature 342, 787-790.
891 Yin, H., Xu, L., Porter, N.A., 2011. Free radical lipid peroxidation: mechanisms and
892 analysis. Chemical Review 111, 5944-5972.
893

APPENDIX

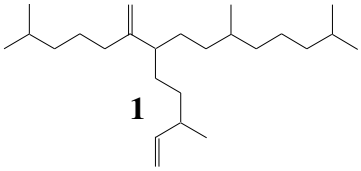

1

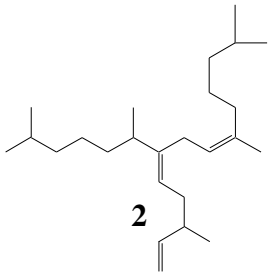

2

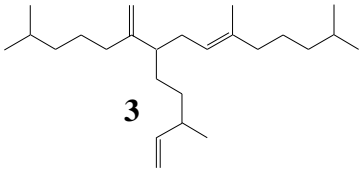

3

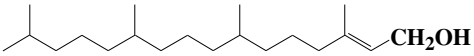

4

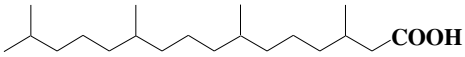

5

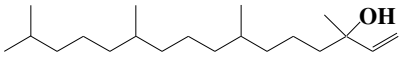

6

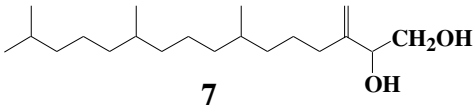

7

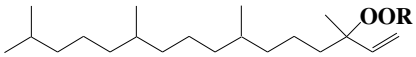

8

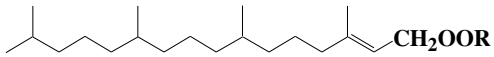

9

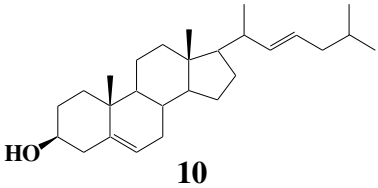

10

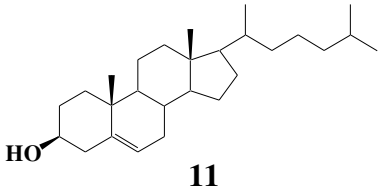

11

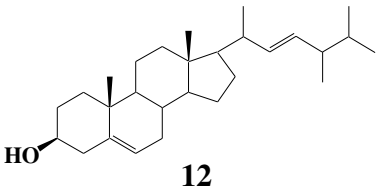

12

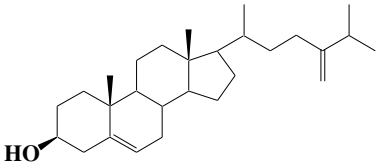

13

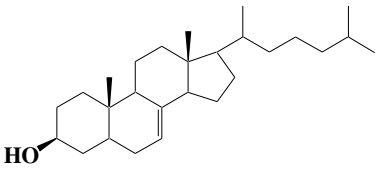

14

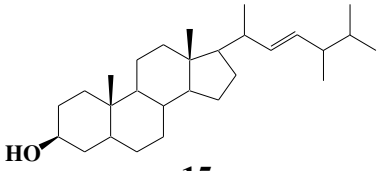

15

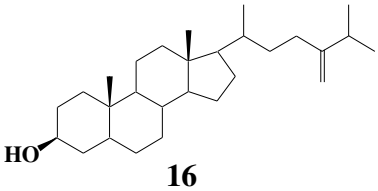

16

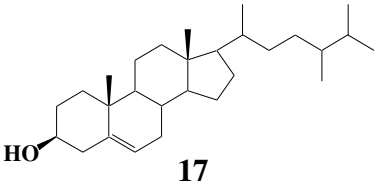

17

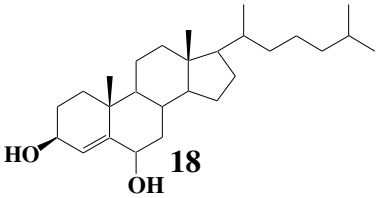

18

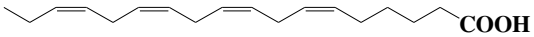

19

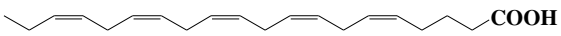

20

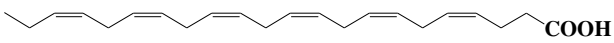

21

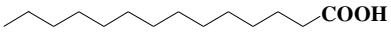

22

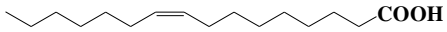

23

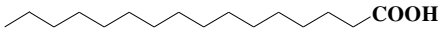

24

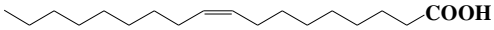

25

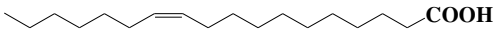

26

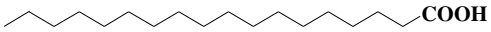

27

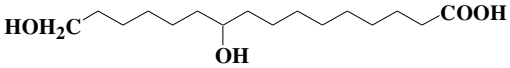

28

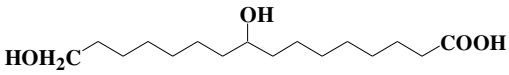

29

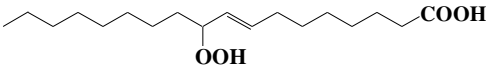

30

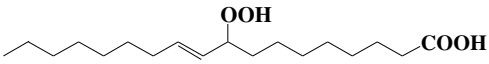

31

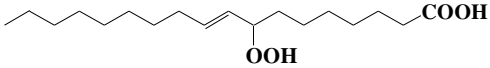

32

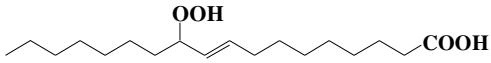

33

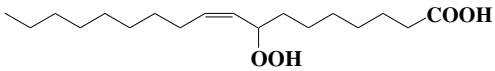

34

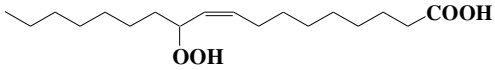

35

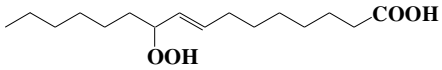

36

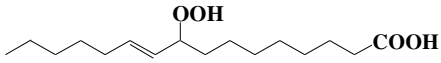

37

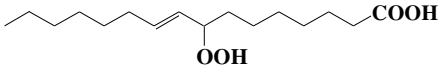

38

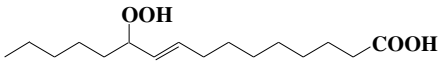

39

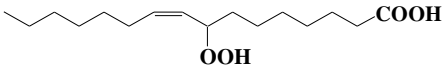

40

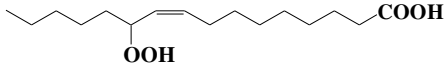

41

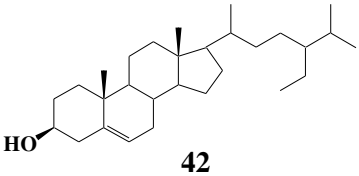

42

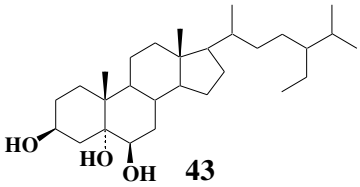

43

895

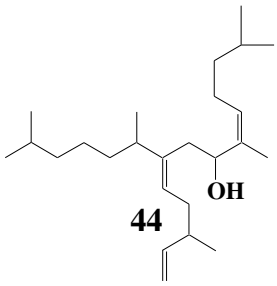

44

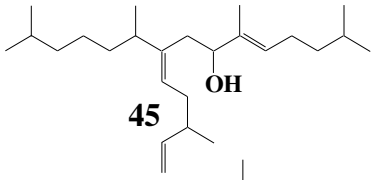

45

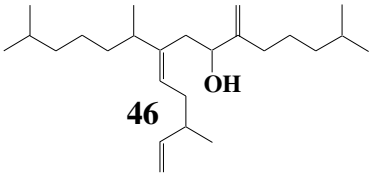

46

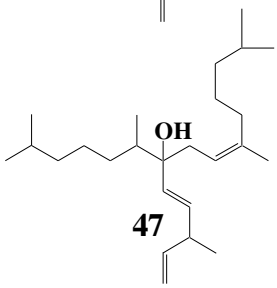

47

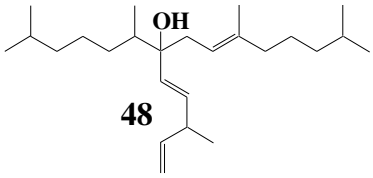

48

896

897 **FIGURE CAPTIONS**

898

899 Figure 1. Summary map showing sampling locations (CB = Commonwealth Bay).

900

901 Figure 2. Proposed pathways for autoxidation of chlorophyll phytyl side chain.

902

903 Figure 3. Photooxidation percentages of *epi*-brassicasterol (**12**), 24-methylenecholesterol
904 (**13**) and chlorophyll in the CTD samples collected at the stations selected for lipid
905 oxidation product analyses. The very low photooxidation percentages of sterols in the
906 samples collected at the station 32 were not included in this figure.

907

908 Figure 4. Photo- and autoxidation percentages of palmitoleic (**23**) and oleic (**25**) acids in
909 the CTD samples collected at the stations selected for lipid oxidation product analyses. The
910 weak oxidation percentages of palmitoleic acid in the samples collected at the station 32
911 are given in Table 3.

912

913 Figure 5. MRM chromatograms (*m/z* 213 → 117, *m/z* 213 → 123 and *m/z* 213 → 157) for
914 standard oxidation products of HBI III (**2**) (A) and CB phytoplanktonic sample collected in
915 Commonwealth Bay (B).

916

917 Figure 6. MRM chromatograms (*m/z* 295 → 93, *m/z* 295 → 107 and *m/z* 295 → 183) for
918 standard oxidation products of the HBI III (**2**) (A) and CB phytoplanktonic sample
919 collected from Commonwealth Bay (B).

920

921 Figure 7. Conceptual scheme summarizing sedimentation and degradation of ice algae and
922 open water phytoplankton in east Antarctica. Note that in some cases the increase of the
923 ratio $IPSO_{25}$(**1**)/HBI III (**2**) with depth may be due to the faster sedimentation rate of
924 aggregated sympagic algae relative to open water phytoplankton and in other cases to an
925 intense photooxidation (in the euphotic layer) or autoxidation (in the entire water column
926 and in the oxic layer of sediments) of HBI III (**2**).

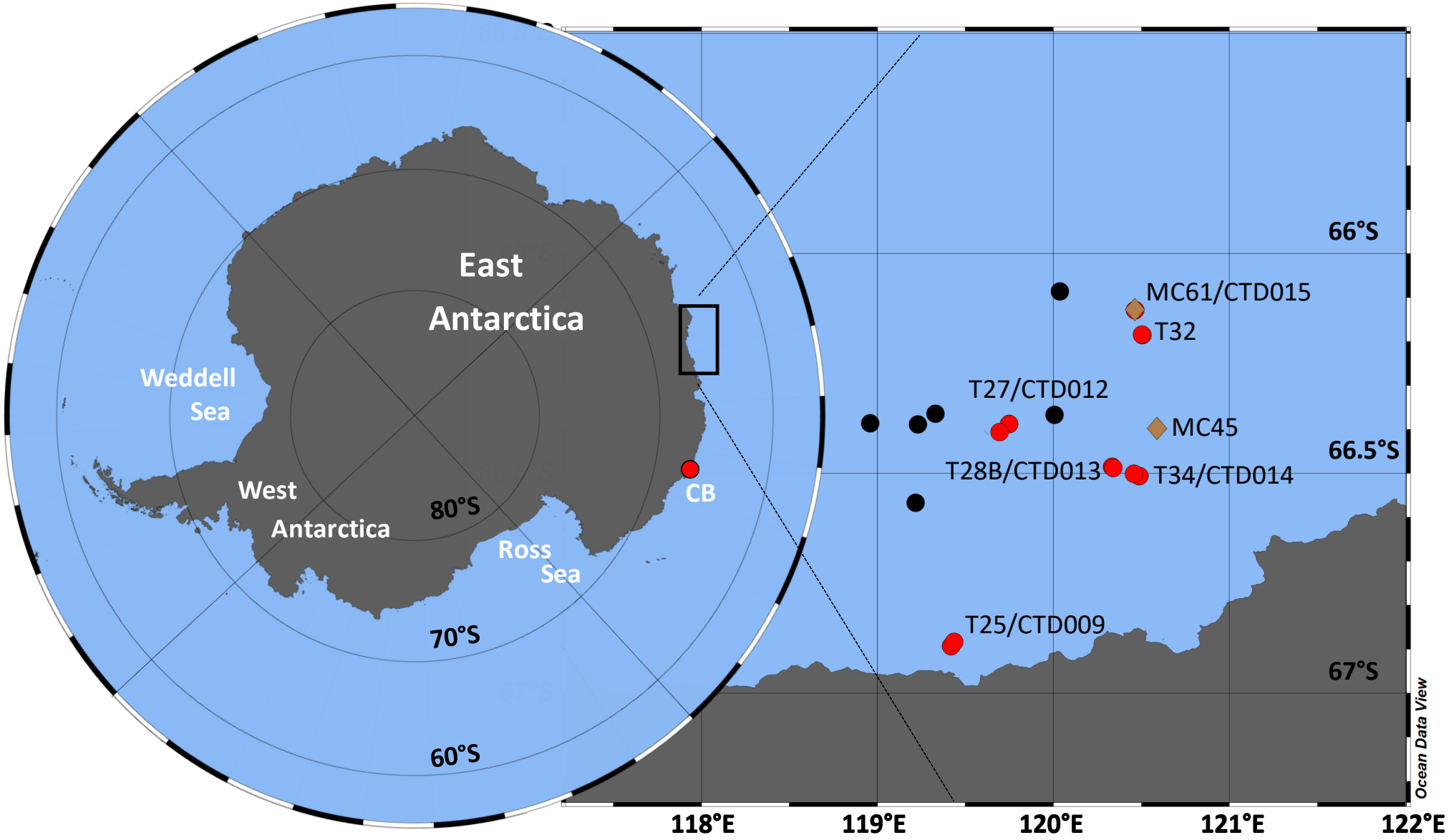

Detailed lipid analysis (oxidation products)

Other CTD stations (native lipids only)

Sediments (Megacores)

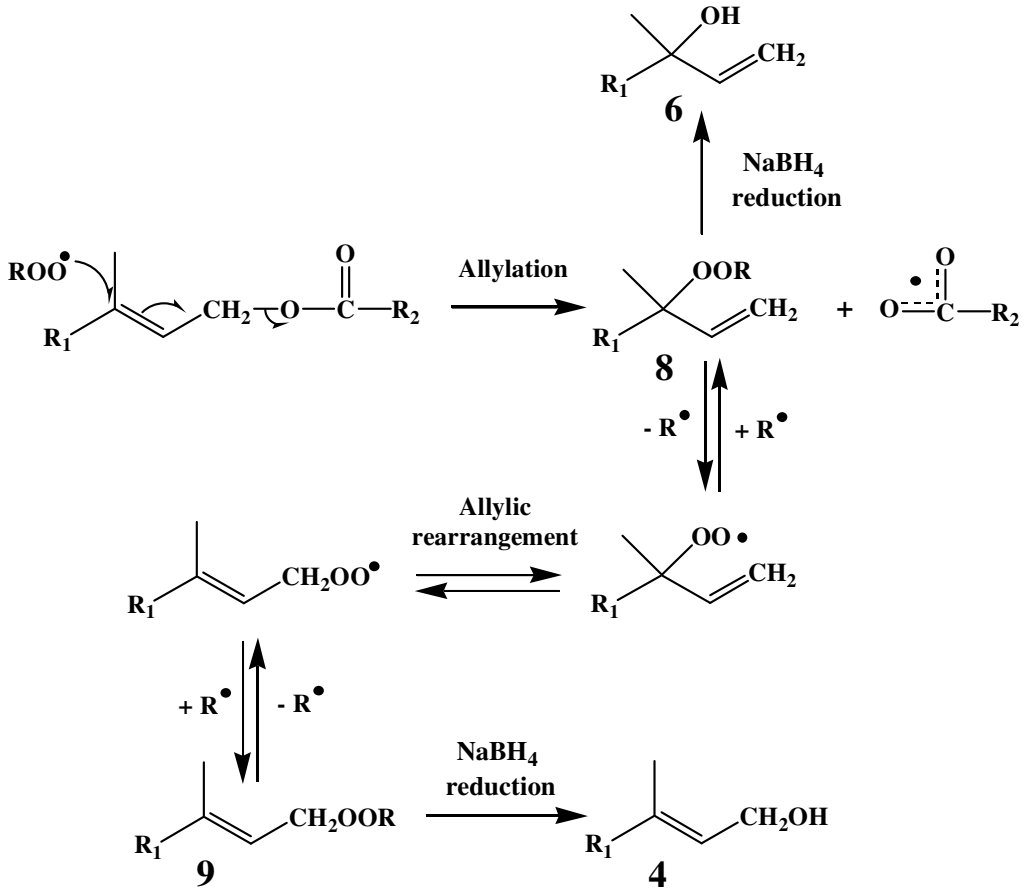

R_1 = 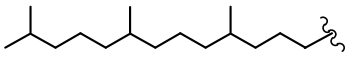

R_2 = 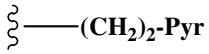

Pyr = More or less oxidized tetrapyrrolic structure

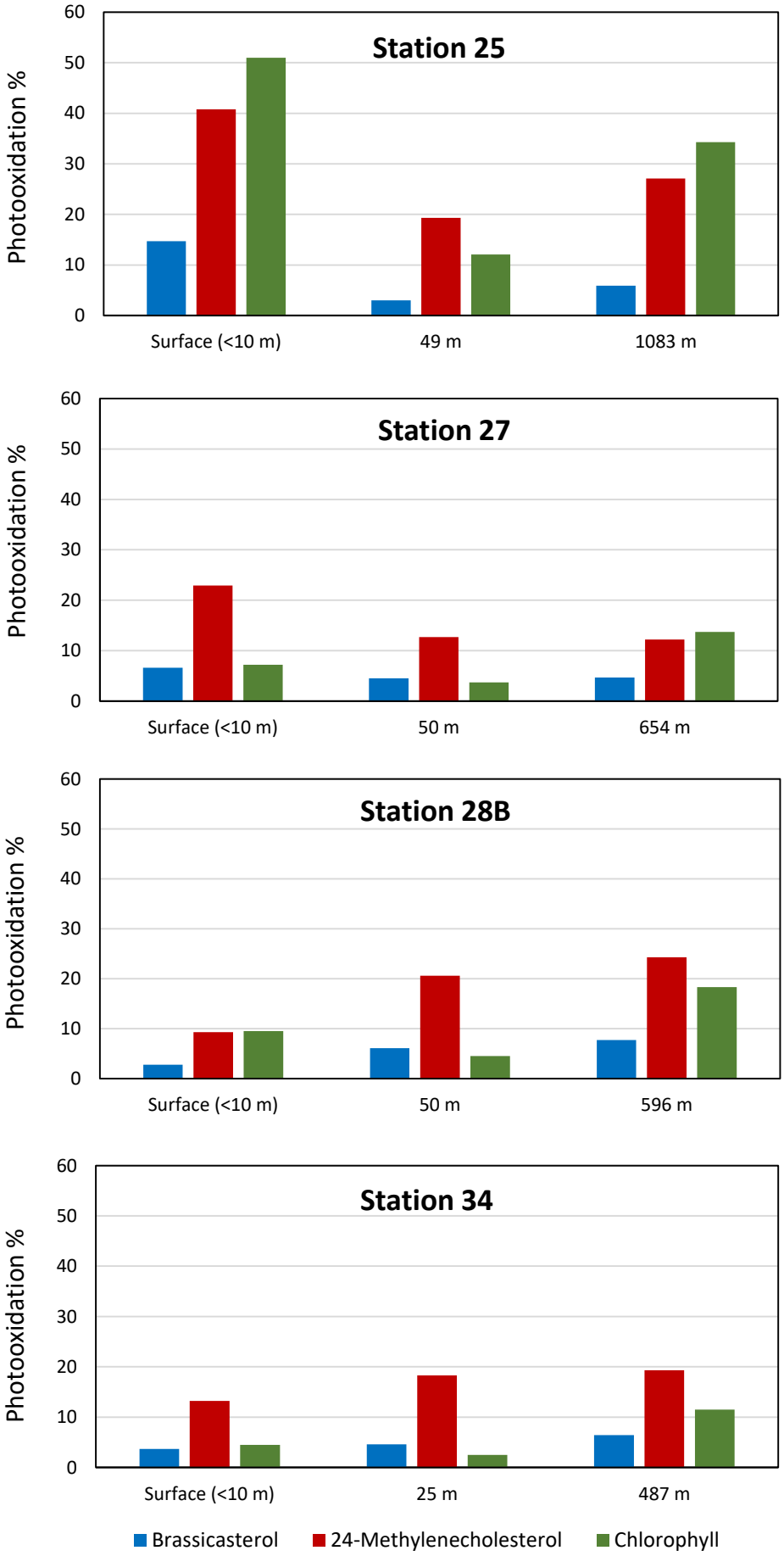
Station 25
Photooxidation %
60
50
40
30
20
10
0
Surface (<10 m)
49 m
1083 m
Station 27
Photooxidation %
Surface (<10 m)
50 m
654 m
Station 28B
Photooxidation %
Surface (<10 m)
50 m
596 m
Station 34
Photooxidation %
Surface (<10 m)
25 m
487 m
Brassicasterol
24-Methylenecholesterol
Chlorophyll

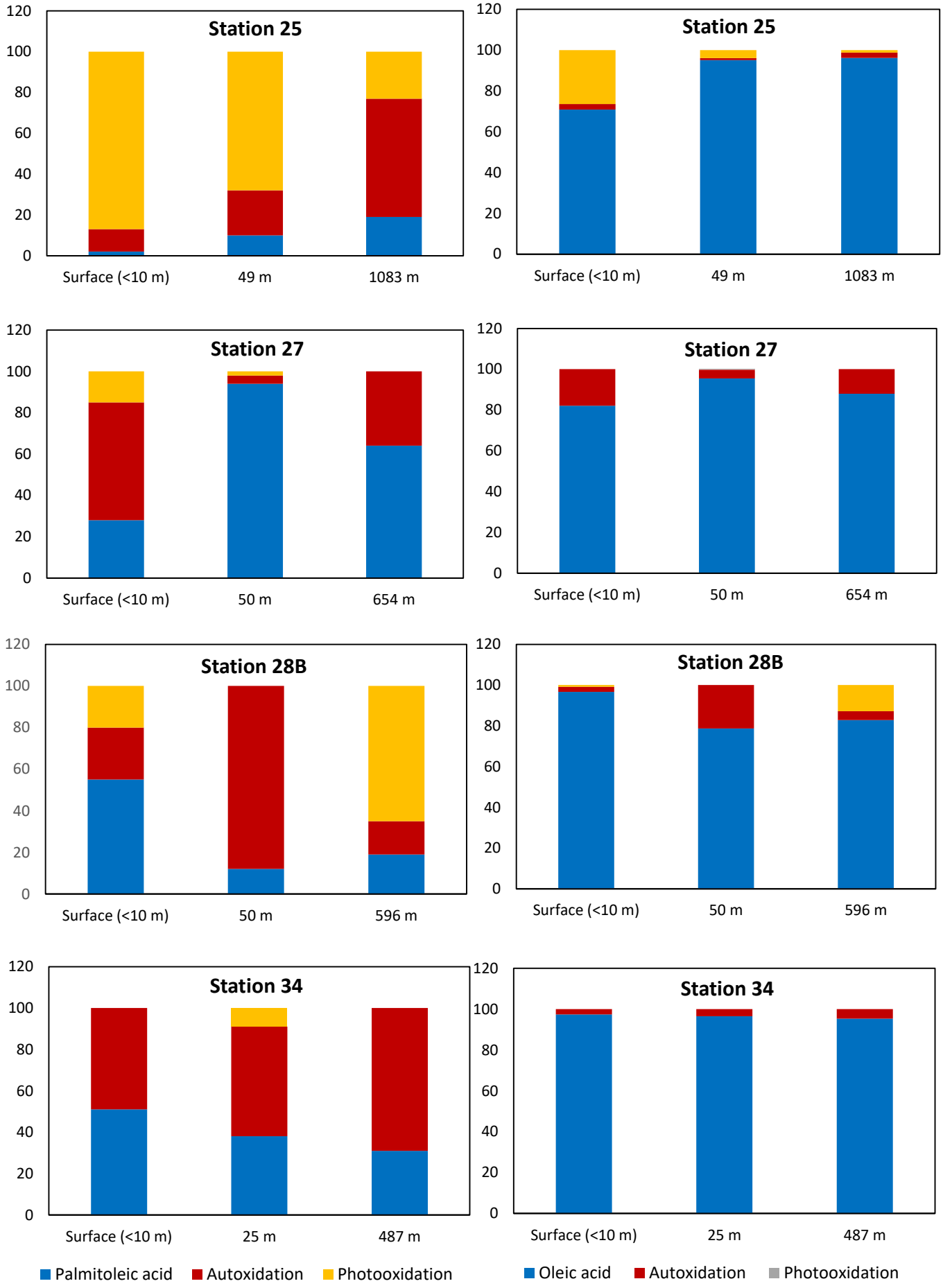
Station 25
Station 25
Station 27
Station 27
Station 28B
Station 28B
Station 34
Station 34
120
100
80
60
40
20
0
Surface (<10 m)
49 m
1083 m
50 m
654 m
596 m
25 m
487 m
Palmitoleic acid
Autoxidation
Photooxidation
Oleic acid
Autoxidation
Photooxidation

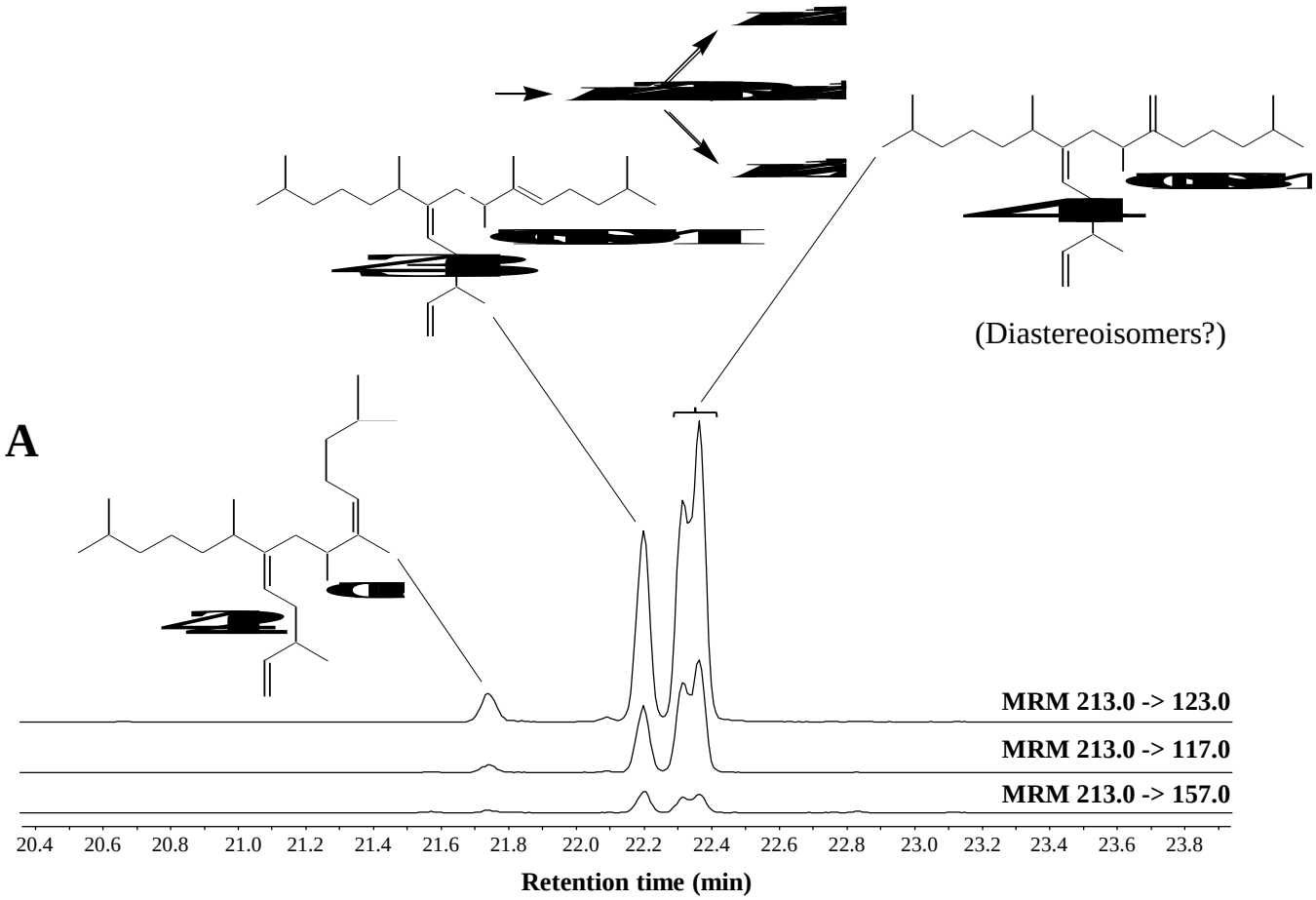
(Diastereoisomers?)
A
MRM 213.0 -> 123.0
MRM 213.0 -> 117.0
MRM 213.0 -> 157.0
20.4 20.6 20.8 21.0 21.2 21.4 21.6 21.8 22.0 22.2 22.4 22.6 22.8 23.0 23.2 23.4 23.6 23.8
Retention time (min)

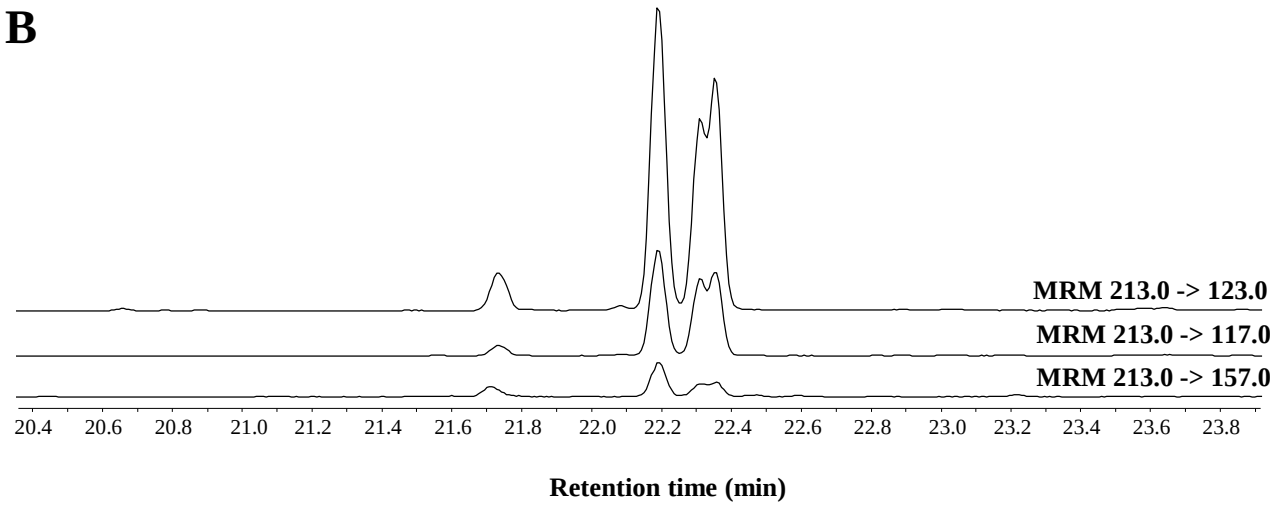
B
MRM 213.0 -> 123.0
MRM 213.0 -> 117.0
MRM 213.0 -> 157.0
20.4 20.6 20.8 21.0 21.2 21.4 21.6 21.8 22.0 22.2 22.4 22.6 22.8 23.0 23.2 23.4 23.6 23.8
Retention time (min)

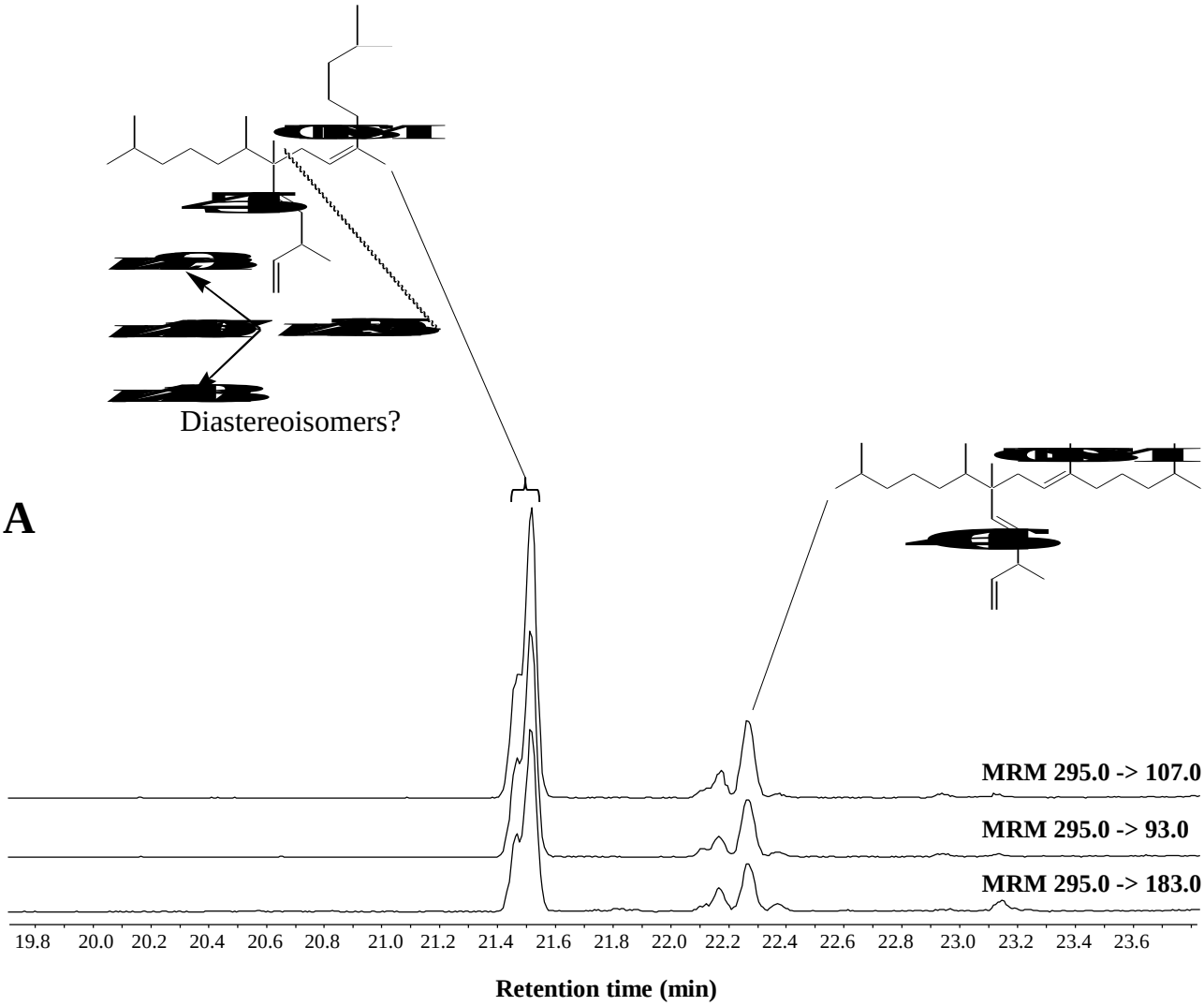
Diastereoisomers?
A
MRM 295.0 -> 107.0
MRM 295.0 -> 93.0
MRM 295.0 -> 183.0
19.8 20.0 20.2 20.4 20.6 20.8 21.0 21.2 21.4 21.6 21.8 22.0 22.2 22.4 22.6 22.8 23.0 23.2 23.4 23.6
Retention time (min)

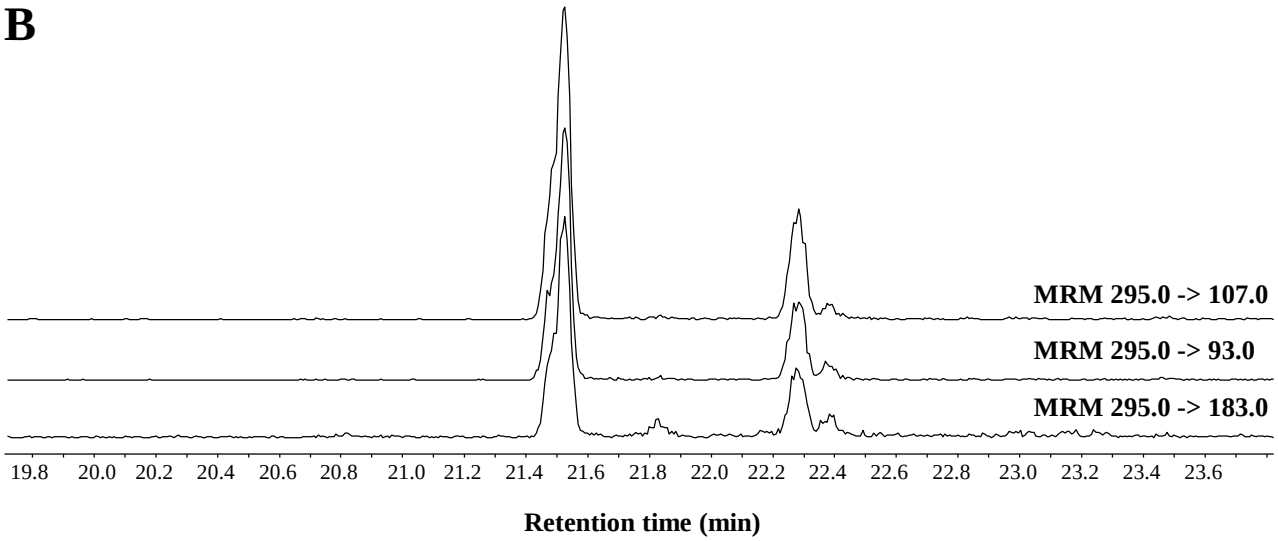
B
MRM 295.0 -> 107.0
MRM 295.0 -> 93.0
MRM 295.0 -> 183.0
19.8 20.0 20.2 20.4 20.6 20.8 21.0 21.2 21.4 21.6 21.8 22.0 22.2 22.4 22.6 22.8 23.0 23.2 23.4 23.6
Retention time (min)

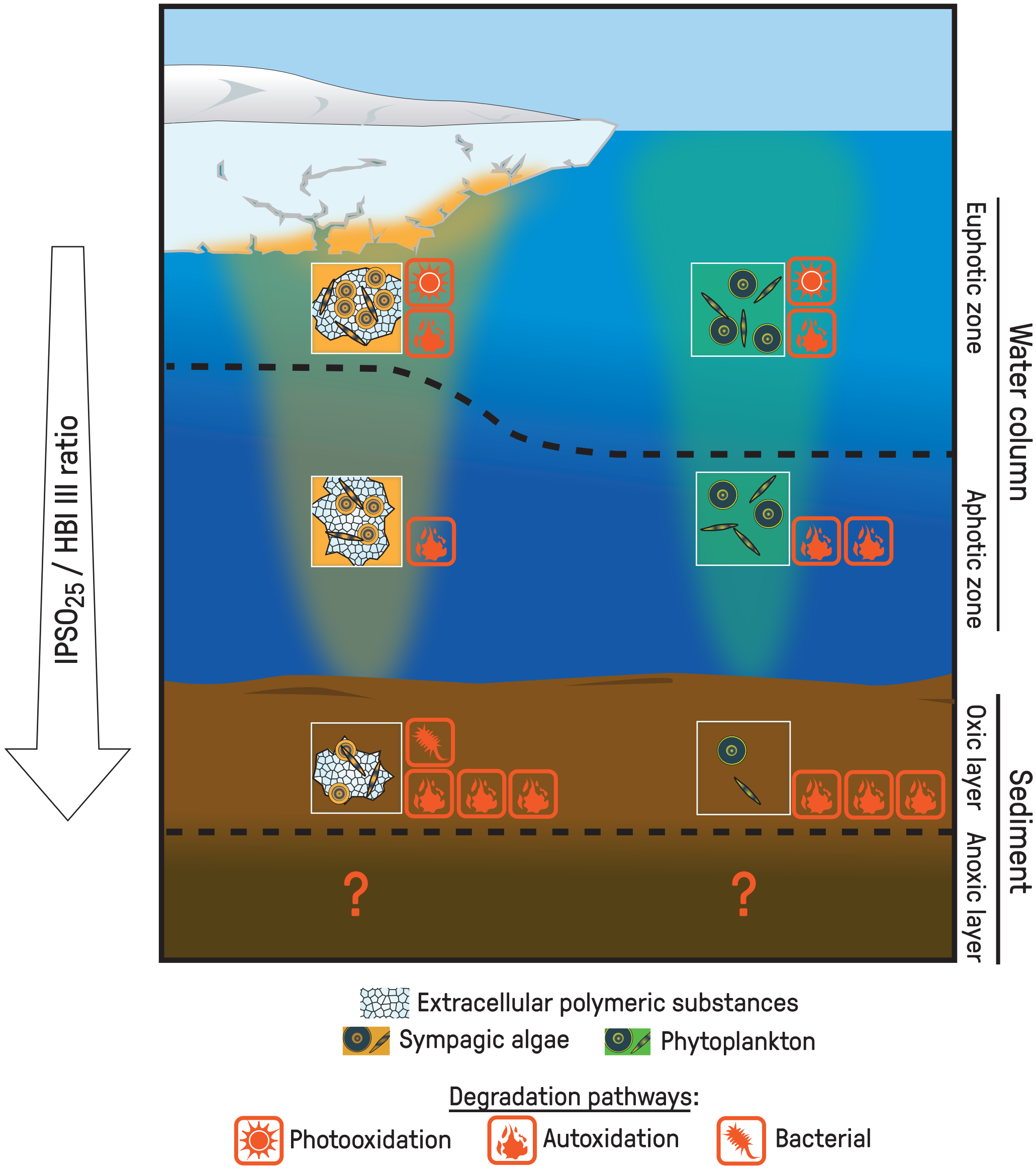
Water column
Euphotic zone
Aphotic zone
Sediment
Oxic layer
Anoxic layer
?
?
IPSO25 / HBI III ratio
Extracellular polymeric substances
Sympagic algae
Phytoplankton
Degradation pathways:
Photooxidation
Autoxidation
Bacterial

Table 1

Different indicators measured at the five stations selected for lipid degradation analyses.

Station	Depth (m)	$IPSO_{25}$ (**1**)/ HBI III (**2**)	Cuticular waxes[a]/ palmitic acid (**24**)	*Epi*-brassicastanol (**12**)/ *epi*-brassicasterol (**16**)	(Palmitoleic acid (**23**)+ ox[b])/ palmitic acid (**24**)	Isophytol (**6**)/ phytol (**4**)
25	<10	0.21	0	0.24	30.91	0.45
25	49	0.26	0	0.20	3.42	1.64
25	1083	2.57	0	0.32	1.65	0.60
27	<10	0.26	0.07	0.17	1.82	0
27	50	0.14	2.15	0.21	0.42	0.01
27	654	1.74	0	0.29	0.25	0.08
28B	<10	0.51	0.02	0.14	1.01	0.30
28B	50	0.44	0.03	0.24	3.11	0.06
28B	596	1.61	0	0.16	4.02	0.20
32	<10	0.21	0	0.10	0.05	0.13
32	40	0.37	0	0.09	0.08	0.08
32	563	0.88	0	0.17	0.02	0.07
34	<10	0.25	0.04	0.14	1.11	0.04
34	25	0.21	1.23	0.17	1.10	0.05
34	487	1.54	0	0.28	1.36	0.03

[a] Mixtures of 9,16-dihydroxyhexadecanoic (**29**) and 10,16-dihydroxyhexadecanoic (**28**) acids

[b] Photo- and autoxidation products

Table 2

Comparison of the ratio **1/2** and the autoxidation state of some other algal lipids in SPM and underlying sediments. See Fig. 1 for sample locations.

Station – sample type	Depth (m)	$IPSO_{25}$ (**1**)/ HBI III (**2**)	Sitosterol (**42**) autoxidation %	Palmitoleic acid (**23**) autoxidation %	*(F. curta + F. cylindrus) / F. kerguelensis*
T32 – SPM	<10	0.2	0	1.3	20.6
CTD015 – SPM	40	0.4	0	9.3	18.8
CTD015 – SPM	563	0.9	0	21.8	8.0
MC61 – overlying water	579	1.6	*	*	0.5
MC61 – diatomaceous 'fluff'	579	2.6	*	*	N/A
MC61 – sediment (1–2 cm)	579	7.5	28.4	53.4	0.7
MC45 – sediment (1–2 cm)	538	11.3	46.3	51.6	0.8

* - not measured
N/A - abundances too low

Table 3

Percentage[a] of oxidation products of HBI III (**2**) detected after $NaBH_4$-reduction of filtered phytoplankton from Commonwealth Bay (East Antarctica)

Sample	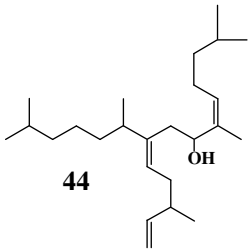 **44**	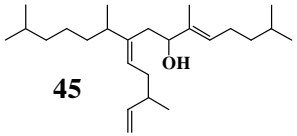 **45**	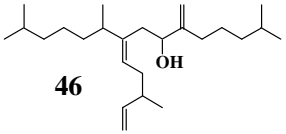 **46**	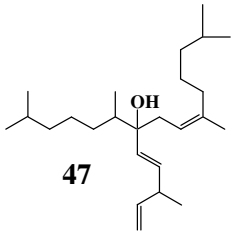 **47**	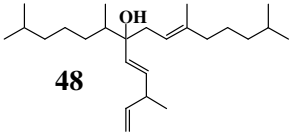 **48**
CB	0.6	9.1	11.2	10.2	5.1
AS607	b	53.4	71.2	65.1	52.7
AS608	10.4	43.6	96.4	9.1	32.7

[a] Relative to the residual parent HBI
[b] Coelution problem

Table 4

Relative percentages of intact hydroperoxides and their ketonic and alcoholic degradation products measured in the case of the main HBI oxidation products present in phytoplankton from Commonwealth Bay (East Antarctica) (CB sample).

X-	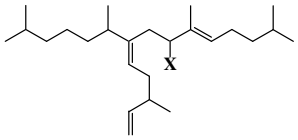	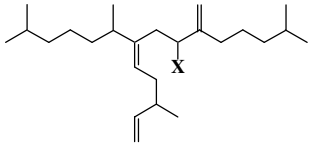	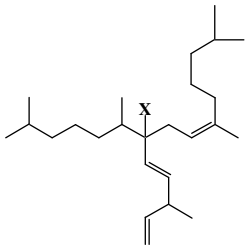	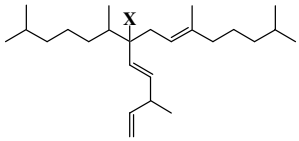
HO-	18	22	21	45
O=	1	3	-	-
HOO-	81	75	79	55